Klaudijus Natys

Process Failure Detection in Fused Filament Fabrication with Internal Data

Master's thesis in Sustainable Manufacturing
Supervisor: Ivanna Baturynska
Co-supervisor: Oleksandr Semeniuta
June 2021

Master's thesis

NTNU
Norwegian University of Science and Technology
Faculty of Engineering
Department of Manufacturing and Civil Engineering

NTNU
Norwegian University of
Science and Technology

Klaudijus Natys

Process Failure Detection in Fused Filament Fabrication with Internal Data

Master’s thesis in Sustainable Manufacturing
Supervisor: Ivanna Baturynska
Co-supervisor: Oleksandr Semeniuta
June 2021

Norwegian University of Science and Technology
Faculty of Engineering
Department of Manufacturing and Civil Engineering

NTNU
Norwegian University of
Science and Technology

Abstract

Additive manufacturing (AM) such as fused filament fabrication (FFF) is a disruptive technology that introduces the possibility to manufacture products in new ways. However, it is facing challenges in terms of product quality and process failures due to the complexity of controlling FFF process. This has resulted in a considerable amount of research around the monitoring systems of FFF. Nevertheless, research is primarily focused on the implementation of external sensors rather than using internal data from FFF machine. Therefore, this study aims at investigating the potential of acquiring internal data for the possibility of detecting process failures. Studied machines are Original Prusa i3 MK3S, Markforged Mark Two, and Ultimaker 3 Extended. Experimental work consisted of creating a data acquisition system based on existing systems, printing and data acquisition. Lastly, the printed models from each machine were measured in a coordinate measuring machine (CMM). Where the methods for acquiring the data were the use of application programming interface (API) and web scraping. Additionally, data analysis was performed from acquired data in order to analyze the quality of the data.

The results of the study show that it is possible to acquire internal data from machines, which include not just sensory data, but also additional machine data. However, in order to acquire the data, there is a need for communication with the FFF system, where only two of three studied machines provided the possibility. To establish communication with the last machine it was needed for additional hardware such as Raspberry Pi running software such as OctoPrint. Additionally, the type of data and quality of acquired data varied from machine to machine. The data acquired for each machine provided the possibility to identify patterns in form of temperature fluctuation at specific moments during the printing process. However, it was not found any relation between deviations in CMM measurements and the acquired data. Moreover, based on the listed process failures and acquired data, it could be possible to detect some process failures, however, a further study of running machines to failure would be required in order to confirm it.

Sammendrag

Additiv produksjon (AM) slik som smeltet filamentfabrikasjon (FFF) er en disruptiv teknologi som introduserer muligheten til å produsere produkter på nye måter. Imidlertid står den ovenfor utfordringer når det kommer til produktkvalitet og prosessfeil på grunn av kompleksiteten av å kontrollere en FFF prosess. Dette har resultert i en betydelig mengde med forskning rundt overvåkningssystemene for FFF. Likevel er forskningen primært fokusert på implementeringen av eksterne sensorer heller enn å bruke intern data fra FFF maskiner. Derfor sikter denne studien seg mot å undersøke potensiale for å innhente data for muligheten for å oppdage prosessfeil. De studerte maskinene er Prusa i3 MK3S, Markforged Mark Two, og Ultimaker 3 Extended. Det eksperimentelle arbeidet besto av å lage et datainnsamlingssystem basert på eksisterende systemer, printing og datainnhenting. Til slutt var de printeded modellene fra hver maskin målt in en koordinatmålemaskin (CMM). Metodene brukt for innhenting av data var bruken av programmeringsgrensesnitt (API), og nettskraping. I tillegg var en dataanalyse utført fra de innhentede dataene for å analysere kvaliteten på dataene.

Resultatene av studien viser at det er mulig å innhente intern data fra maskinene, som ikke bare inkluderer sensorisk data, men også ytterlige data fra maskinen. For å kunne hente inn dataen er det behov for kommunikasjon med FFF-systemet, der bare to av tre studerte maskiner ga muligheten. For å etablere kommunikasjon med den siste maskinen var det nødvendig med ekstra maskinvare som Raspberry Pi, som kunne kjøre en programvare OctoPrint. Tilgjengelig data og kvaliteten på innhentede data varierte fra maskin til maskin. Dataene som var innhentet fra hver maskin ga muligheten til å identifisere mønstre i form av temperatursvingninger på spesifikke hendelser i løpet av printerprosessen. Imidlertid ble det ikke funnet noen sammenheng mellom avvik i CMM-målinger og den innsamlede dataen. Videre, basert på listede prosessfeil og innhentede data, kan det være mulig å oppdage noen prosessfeil, men det ville kreve videre undersøkelser av å kjøre maskiner til de svikter for å kunne bekrefte dette.

Acknowledgments

I would like to express my sincere gratitude to my supervisor Ivanna Baturynska for providing me with thorough supervision through the entire thesis, which kept me motivated with my work. I would also thank my co-supervisor Oleksandr Semeniuta for additional input from a different perspective. Additionally, I am also very thankful to both supervisors for connecting me with Christian Dalheim Øien from SINTEF and Emma Østerbø from MTNC.

Big thank you to everyone from MTNC, that welcomed me and gave me the possibility to work at your premises with your machines.

Lastly, I would like to truly thank my dear Daniela Kristiansen for always supporting and believing in me through the good and bad days.

Table of Contents

List of Figures

List of tables

List of Abbreviations

AM	Additive manufacturing
FFF	Fused filament fabrication
RQ	Research question
CMM	Coordinate measuring machine
API	Application programming interface
3DP	3D printing
COVID-19	Coronavirus disease 2019
SVM	Support vector machine
BPNN	Back propagation neural network
LS-SVM	Least squares support vector machine
PID	Proportional, integral, derivative
RP	Rapid prototyping
STL	Standard triangle language
CAD	Computer-aided design
ABS	Acrylonitrile butadiene styrene
PLA	Polylactic acid
PC	Poly carbonate
HIPS	High impact polystyrene
TPU	Polyurethane
PET	Polyethylene terephthalate
PETG	Polyethylene terephthalate glycol
PEEK	Polyether ether ketone
PLA-g-MA	Polylactic acid graft maleic anhydride
SEBS	Styrene-ethylene butylene styrene
SMA	Styrene-maleic anhydride copolymer
CM	Condition monitoring
REST	Representational state transfer
HTTP	Hypertext transfer protocol
JSON	JavaScript object notation
URI	Uniform Resource Identifier
WWW	World wide web
DOM	Document object model
CSS	Cascading style sheets
XPath	XML path language
SFI	Centre for Research-based Innovation
MTNC	Manufacturing Technology Norwegian Catapult Centre
IR	Infrared
USB	Universal serial bus

1 Introduction

Additive manufacturing (AM) technology is one of the most recent manufacturing technologies, which was introduced in the 1980s. Since then the growth of AM, also commonly referred to as 3D printing (3DP) has been increasing at a rapid paste (JEMGHILI, TALEB and MANSOURI, 2020). It is a type of formative manufacturing technology that is capable to manufacture 3-dimensional objects with few geometrical restrictions (Kretzschmar *et al.*, 2018). This introduces the possibility to produce products in a new way, which was challenging or not possible before with conventional manufacturing processes (JEMGHILI, TALEB and MANSOURI, 2020). AM is considered to be a disruptive technology, due to its characteristics of ability to manufacturing products from digital models, and a possibility to produce customized products without much complexity. Which would have an impact on various processes such as production, supply chain, logistics, and product life cycle planning (van Bracht, Kleer and Piller, 2017).

An example of AM capabilities of adapting to changes showed during the coronavirus disease 2019 (COVID-19) when health and medical sectors had a shortage of equipment. During COVID-19 numerous product designs such as face masks frames, nasal swabs, oxygen valves, were developed and made available as open-source. Which provided the possibility for companies to manufacture these products based on the models. Where companies that participated were Volkswagen, Prusa Research, Stratasys, Formlabs, and many more (Mwema and Akinlabi, 2020).

In this thesis work, the focus is set only on the material extrusion type of additive manufacturing, also called fused filament fabrication (FFF), in particular desktop FFF. Where FFF has been used in a wide area of application within civil, biomedical, medical (Fu *et al.*, 2020), aerospace (Brenken *et al.*, 2018), automotive industries, etc (Osswald, Puentes and Kattinger, 2018). Although it has been several decades since it was introduced, AM technology has yet to reach its maturity for industrial purposes (Kretzschmar *et al.*, 2018). The challenges in FFF are within product quality, robustness, material properties, controllability, etc (Wu, Yu and Wang, 2019). This is primarily due to the complexity of controlling the process (Kretzschmar *et al.*, 2018). In FFF these challenges commonly result in the need for trial-and-error methods in order to meet the desired product quality (Wu, Yu and Wang, 2019). Which is primarily done by offline optimization of process parameters (Liu *et al.*, 2019). However, due to FFF being a complex process in itself with high variation, optimal process parameters might still be insufficient. Therefore, for some process parameters, it might be required of continuous changes during the process. To avoid this trial and error approach and have the ability to understand when the process parameters need to be changed continuously, there is firstly a need for data (Liu *et al.*, 2019).

Therefore, to assess these challenges, there has been a considerable amount of research on implementing external sensors for online monitoring systems in FFF (Liu *et al.*, 2019). The research about monitoring FFF process failures shows that it is monitored both product quality, but also machine failures. Where the failures could be caused by material runout, over/under-extrusion, temperature variation, process parameters, material quality, vibration, etc. Where numerous types of external sensors have been employed to monitor both states such as acoustic emission, encoders, thermocouples, optical and thermal cameras, current sensors, accelerometers, and many more (Fu *et al.*, 2021). In addition to sensors, techniques such as coherent gradient sensing and physics-based compressive sensing, and sensor fusion approach were applied (Yi, Lee and Cho, 2018). Finally to make use of the data to create some predictive models, commonly a form of machine learning algorithms are applied (Fu *et al.*, 2021). Wu, Wang and Yu (2016) observed feeding and extrusion system with a non-intrusive acoustic emission sensor. Where support vector machines (SVM) were used to classify failures such as material runout, material flow, and extrusion blockage. Jin, Zhang and Gu (2019) used camera sensor with computer vision and deep learning techniques to monitor real-time extrusion states of over and under-extrusion. Whereas Saluja, Xie and Fayazbakhsh (2020) used a camera with computer vision system and deep learning algorithms to identify warping defects. Additionally, a closed-loop system was implemented to stop the FFF process if warping was identified. Malekipour, Attoye and El-Mounayri (2018) used an infrared (IR) camera to observe temperature distribution during different deposition layers in real-time. Where the thermal interaction such as thermal stress between layers has an impact on failures such as warping and curling. Li, Y. *et al.* (2019) used two vibration sensors to detect process failure such as extruder jam, material leakage, and warping where machine learning methods such as SVM, back propagation neural network (BPNN), and least squares support vector machine (LS-SVM) were applied. Rao *et al.* (2015) studied effect of the use of heterogeneous sensors to detect abnormal extrusion and nozzle clogging. In the study, it was used thermocouples, IR temperature sensor, borescope and accelerometers. Anderegg *et al.* (2019) studied FFF machines nozzle state with help of thermocouples and pressure sensor. Their study shows that temperature fluctuation significantly affects the pressure build up inside the nozzle which causes defects such as material leaking from nozzle, inconsistent extrusion, and stringing. With the data from the sensors, they were able to implement a proportional, integral, derivative (PID) system which controls the temperature fluctuation and reduces the pressure inside the nozzle. While Li, Z. *et al.* (2019) used thermocouples, IR temperature sensor, and accelerometer sensors to investigated product quality during FFF process in form of surface roughness. Moretti, Bianchi and Senin (2020b) used camera, encoders and thermocouple sensors in order to detect process failures such as misalignments, nozzle clogging. However, the same authors also stated that in order to acquire maximize the external sensor data quality, a redesign of FFF machines might be needed.

Although the literature shows that external sensors can observe a specific phenomenon of interest, it introduces complexity in form of additional components. While other studies go as far as redesigning the FFF machine to implement sensors. Considering desktop FFF machines are low-cost machines, these modifications, and additional components might result in exceeding machine cost. In addition, FFF machines are built differently, therefore sensor placements from the literature are machine specific. However, FFF machines are already equipped with some sensors. Considering FFF machines contain some sensors, such as temperature sensors, which are some of the process failures influenced by. Nevertheless, there has been found only a single study that investigated the internal sensors within FFF machines, by Liu *et al.* (2016). The study showed also that in addition to sensor data, the machines contain additional internal data which could be valuable in terms of failure detection.

1.1 Research questions

This study aims at investigating the potential of acquiring internal data from FFF machines. Where the goal is to identify if the internal data could provide some value in terms of failure detection of FFF. In order to answer this, it is needed to answer some research questions:

RQ1. What types of internal data exist in FFF machines?

Firstly, there is a need of identifying what type of sensors are present in FFF machines. In addition, like mentioned in the Introduction section, a study by Liu *et al.* (2016) showed that machines contain more than just internal sensor data. Where the additional data could provide data that regular sensors might not be able to capture.

RQ2. What types of internal data are possible to acquire, and how could it be obtained?

To develop a monitoring system, there is a need for data acquisition, therefore RQ2 aims at addressing the possibility of acquiring internal data based on the results RQ1. Additionally, as multiple FFF machines will be studied, it will be investigated the possibility of generalizing the results of data acquisition for all FFF machines.

RQ3. How could internal data alone be used for failure detection in the FFF process, and when are additional sensors required?

RQ3 aims at investigating the possibility of using only internal data for failure detection. The result of that would provide further understanding if external sensors are necessary in order to detect failures in the FFF process.

1.2 Study scope and limitations

This study is valid only for the studied machines which are Original Prusa i3 MK3S, Ultimaker 3 Extended, and Markforged Mark Two, as illustrated in Figure 1.1. This is because FFF machines are built differently both mechanically and firmware-wise, which could potentially cause results to differ for other FFF machines. Additionally, this study will utilize already existing systems to access the data. This is due to the complexity and time requirements to develop new systems, especially for three different FFF machines. Lastly, this study will contain data acquisition methods over a network, and since the main focus is investigating the potential use of internal data of FFF machines. It is therefore not considered the cyber-security aspect of the data acquisition methods. Lastly, due to the large selection of available material on the market for the FFF process, material-related aspects are not investigated in this work.

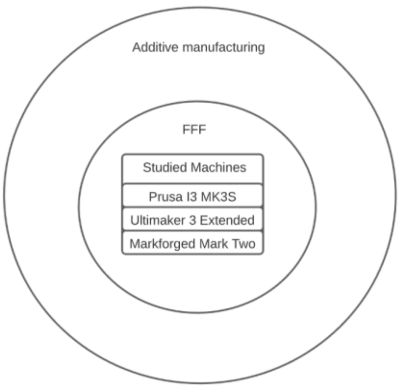

Figure 1.1 Studied FFF machines

1.3 Thesis outline

Thesis is split into six chapters, where the following chapter will be presenting:

Chapter 2 provides theoretical knowledge to support this thesis background. Firstly, generic about AM and its technologies will be introduced. Then it will be presented about FFF, in form of how FFF works and its process flow. Additionally, it will be looked into what impacts the process in terms of process parameters, failures, and materials. Lastly, it will be presented about monitoring systems nowadays, but also about specific data acquisition methods that will be used in this thesis work.

Chapter 3 describes the methodological approach used which includes methods such as a literature review and experimental work.

Chapter 4 presents the results of this thesis based on research questions. The results are split into three separate sections, according to each RQ.

Chapter 5 is the discussion part, here the results and their meaning will be discussed according to the theoretical background.

Chapter 6 provides the concluding statement of the thesis.

2 Theoretical background

2.1 Additive manufacturing

AM is commonly referred as rapid prototyping (RP) as it provides the possibility to create new objects quickly, without the need of changing machinery tools (Gibson *et al.*, 2014). This introduces the possibility to prototype products in the early stages of development without great expenses at rapid paste as the name suggests. Commonly in traditional manufacturing, to manufacture a part it is needed to have a complete analysis of the part's geometry, which allows understanding of what tools, processes, etc, is needed to manufacture the part. However, in AM the main aspect is knowing the machine's capabilities and basic geometrical data from the model. Although AM is commonly referred to as rapid prototyping, it is not because of the speed of the manufacturing process itself. It is due to the speed of the product development process, as you are using computers to generate models and AM machines that need little to no adjusting to be able to manufacture the models into physical parts. It also provides the possibility to cut down process steps, as no matter what geometrical complexity the part contains, it is still manufactured in a single process. Whereas in traditional manufacturing, the more complex the part contains the more processes it requires to go through to be manufactured (Gibson *et al.*, 2014).

The working principle of AM is made by creating layers where the material is added layer by layer. The result of the layering method introduces the importance of part orientation during the process, as it will influence its properties (Leirmo and Martinsen, 2019a). Where the layers are illustrated in Figure 2.1, the lower the layer height, the finer the quality of the 3d printed part is. However, increasing the number of layers increases the production time, as more layers need to be gone through. Today all commercialized AM technologies utilize this type of layer-based approach, the major difference in different AM technologies is the way the layers are produced, how the layers bond together, and the choice of material (Gibson *et al.*, 2014). Nevertheless, there has been some development of a new type of AM technology, Computed Axial Lithography. This type of technology eliminates layers, as the objects are no longer created layer by layer, instead, the entire geometry is created at once (Kelly *et al.*, 2017). The result of these differences in AM technologies will define the mechanical properties of the parts, dimensional accuracy, amount of post-processing, AM machine size, costs of the entire process, but also how quickly a part can be manufactured (Gibson *et al.*, 2014).

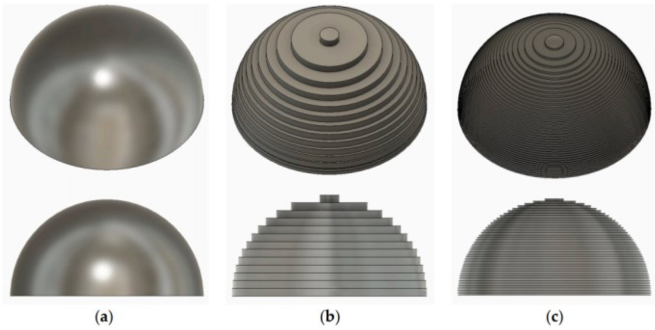

Figure 2.1: Illustration of layers on a sphere (a) ideal shape, (b) illustrates high layer heights, (c) finer layers (Amza, Zapciu and Popescu, 2017)

2.1.1 AM technologies

AM technologies are categorized into seven types: Binder jetting, directed energy deposition, material extrusion, material jetting, powder bed fusion, sheet lamination, vat photopolymerization (ISO/ASTM, 2017). Powder bed fusion utilizes powder which is contained in a build platform as the raw material form to produce the product with thermal energy (ISO/ASTM, 2017). It is used either laser or electron beam to melt or fuse the layers of powder together (Adekanye *et al.*, 2017). Binder jetting uses powder as a material as well, however, instead of thermal energy, it is used a binder agent to bond the powder selectively (Adekanye *et al.*, 2017; ISO/ASTM, 2017). Whereas in material jetting the powder material is selectively deposited instead of a binder agent (ISO/ASTM, 2017). Direct energy deposition uses powder or wire as a material and melting process is through thermal energy with laser or electron beam, where the material is melted continuously as it is being deposited (Adekanye *et al.*, 2017). Sheet lamination is where sheets of material are bonded which creates the part. Vat photopolymerization is where liquid light-sensitive polymer is used as a material in a vat, where it is cured selectively by a light source. In material extrusion or FFF, it is extruded in selected areas through a nozzle (ISO/ASTM, 2017). Table 2.1 provides with a description of some main key advantages and disadvantages of AM technologies. As mentioned in the Introduction chapter, the focus of this study will be on FFF, which will the following 2.2 section go more in detail about.

Table 2.1: Advantages and disadvantages of different AM technologies

AM technology	Advantages	Disadvantages	Source
Powder bed fusion	Good Mechanical Properties Less anisotropy than other AM processes	Rough surfaces Additional post-processing required	(Ligon *et al.*, 2017; Hunter *et al.*, 2020)

Binder jetting	Fast process Multi-material Low-temperature process	Limited strength Rough surfaces	(Ligon *et al.*, 2017)
Material jetting	Fast process Multi-material	Limited material choice	(Ligon *et al.*, 2017; Gibson *et al.*, 2021)
Direct energy deposition	High resolution High dimensional accuracy	Rough surfaces Complex process	(Saboori *et al.*, 2019)
Sheet lamination	Compact machine	Limited materials Low resolution High anisotropy	(Ligon *et al.*, 2017)
Vat photopolymerization	Great surface quality Good precision	Mechanical properties are limited	(Ligon *et al.*, 2017)
Material extrusion	Low-cost machine and materials	Rough surfaces High process temperatures	(Ligon *et al.*, 2017)

2.2 Fused filament fabrication

In Fused filament fabrication (FFF) material is extruded through a preheated nozzle. The material is then laid layer by layer by having the XYZ axis move to selected locations and deposit material (Adekanye *et al.*, 2017). However due to the layered method in FFF, the strength of the object is dependent on the orientation it is processed, as the layered method introduces an anisotropic structure (Aw *et al.*, 2018; Vosynek *et al.*, 2018; Camargo *et al.*, 2019).

Figure 2.2 (a) illustrates generic components FFF machine. The material in form of continuous filament is being fed through a cold end into the hot end, where the filament is heated into a semi-molten state and finally extruded on the build platform through the nozzle. Where the filament diameter is either 1.75mm or 2.85mm (Kuznetsov, Tavitov and Urzhumtcev, 2019). Figure 2.2 (b) illustrates a more detailed overview of the cold and hot end, also called Extruder. Cold end is the feeding system responsible for feeding and retracting filament. It consists of an idler pulley that holds filament in the correct position and with help of a loaded spring presses towards drive gear or a hobbed bolt. Where the driver gear is mounted on an stepper motor also called extruder motor which provides the possibility to feed and retract the filament. Hot end consists of a heat sink, heater block, nozzle, and fans for the heatsink and nozzle. These components aid in a controlled process of heating material to the correct temperature of a semi-molten filament which could be extruded through a nozzle (Fu *et al.*, 2021)

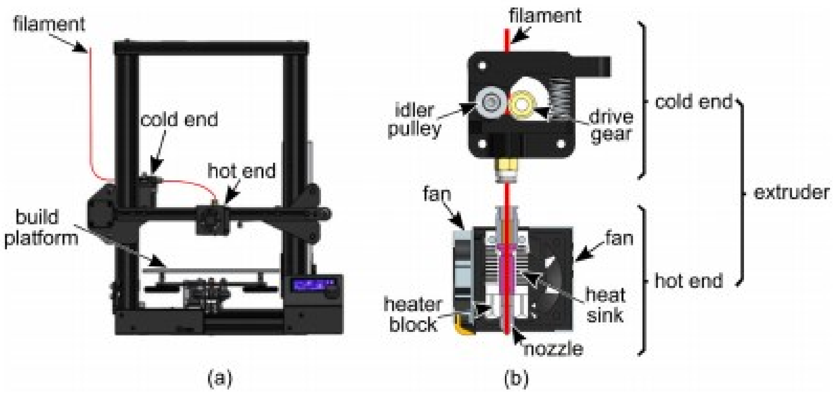

Figure 2.2 (a) Generic components in FFF machine (b) Components of extruder (Fu *et al.*, 2021)

Furthermore, the feeding system placement varies depending on the type of FFF machine. When the feeder is placed distant from the hot end, commonly on machines body frame as illustrated in Figure 2.2 (a). It is called bowden type of extrusion, as it commonly consists of a bowden tube between cold and hot end where the filament is feed through. Additionally, there exists direct extrusion, when the feeder is placed directly over the hot end, similarly as illustrated in Figure 2.2 (b). Both types of extrusion setups have their own benefits and disadvantages (Fu *et al.*, 2021);

- Direct extrusion: Since motors are placed directly over the hot end, less torque is required to control the filament movement, which introduces better extrusion and retraction control. However, since the extruder motor is placed on a moving axis, increased weight adds limitations to the printing speed but also possibility for reduced accuracy in movements (Fu *et al.*, 2021). Examples of machines that are direct extrusion are Original Prusa i3 MK3S (Kuznetsov, Tavitov and Urzhumtcev, 2019), Monoprice Maker Select Plus, Qidi X-Pro, etc (Miller, 2021)
- Bowden extrusion: Increased the ability to print faster and maintain accuracy as the motors are placed on the frame. However, feeding through a longer distance with bowden tube introduces the potential for friction hence more torque is required from the motors. The increased distance between cold and hot end also increased the response time. Additionally, some materials such as abrasive and flexible might wear or tangle up with the bowden setup (Fu *et al.*, 2021). Examples of machines that use the bowden type of extrusion are Ultimaker 2, 3DQ mini, Delta WASP 2040 (Kuznetsov, Tavitov and Urzhumtcev, 2019), but also Ultimaker 3 extended and Markforged Mark Two.

Although in FFF it is possible to manufacture complex geometries, it comes with some limitations. Geometries that contain steep angles or when there are no layers below the next layer are called overhangs (Allen and Trask, 2015). In order to print these geometries, it results in the need for a support structure (Medellín-Castillo and Zaragoza-Siqueiros, 2019). However, the support structure in essence is a waste of material as it will be required to be removed and has no real meaning for the final product. In addition objects with support structures increase the production time (Mwema and Akinlabi, 2020).

One of the main limiting factors with FFF is the surface roughness it creates. This is a result of the layering method in AM where the consequent layers need to fuse with previous layers, which is known as a stair-stepping effect, as illustrated in Figure 2.3. Comparing to computer-aided design (CAD) surface, these stairs introduce surface roughness in the range of micrometers. To some extent it possible to control the stair-stepping effect through process parameters, with the cost of production time. However, for some applications that might not be enough, which would result in the need for post-processing. If not treated it can lead to the possibility of moisture absorption, which could affect the properties of the object. Post-processing of FFF parts could be done chemically or mechanically. Most commonly it is used mechanical post-processing methods, including polishing, sanding, machining, abrasion, and barrel finishing. For chemical post-processing, it is used coating, heating, painting, vapor deposition. Whereas the choice of post-processing method highly depends on the application and material of the object (Mwema and Akinlabi, 2020). Additionally, in transition between layers, when the Z-axis moves to the next layer, nozzle stays still for a moment. During that moment, nozzle leaks some material which introduces a minor seam defect. These defects are natural occurrences in FFF, however, it is possible to control their position in slicing software's (Zapciu, Tasca and Amza, 2018). Another challenge with FFF is that the quality of the process is affected by external factors such as vibration, ambient temperature, and moisture (Khan *et al.*, 2020; Mwema and Akinlabi, 2020).

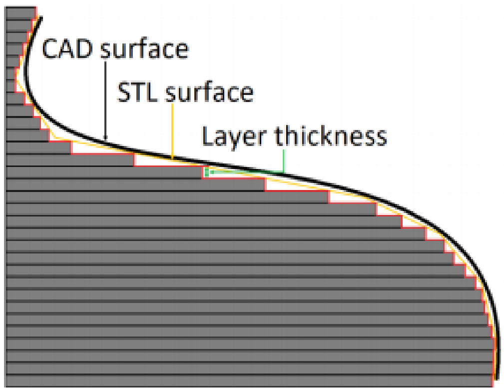

Figure 2.3: Stair stepping effect and STL conversion errors from CAD (Leirmo and Martinsen, 2019a)

FFF contains a considerable number of failures that could occur during the process. These types of failures will be presented in section 2.2.6. Nevertheless, due to the complexity of controlling the process, it could lead to an economically costly process. This is because commonly FFF process has to be manually observed, and if a failure was detected, the processed object usually results in becoming waste, and the FFF process has to be restarted again (Mwema and Akinlabi, 2020).

2.2.1 FFF process steps

Figure 2.4 illustrates the FFF process steps. (1) To be able to 3d print you need a virtual representation of the part that completely describes the external geometry. This can be done either using CAD software to create a solid or surface of the model. If the part exists physically, it is also possible to reverse engineer the part by scanning it, such as optical scanners to create the visual model (Gibson *et al.*, 2014).

(2) Once the virtual 3d model is obtained, the model is converted into standard triangle language (STL), which creates a triangular mesh of the CAD model (Leirmo, Semeniuta and Martinsen, 2020). It will describe the model's external surfaces from the CAD model (Gibson *et al.*, 2014).

(3) STL file is then transferred into printer software, often called slicing software. Here are all the process parameters selected, which include things such as printing speed, type of material, models geometry size, etc (Ravi and Shiakolas, 2021). Once the model parameters are set, it is then exported into a set of commands that the machine can understand, most commonly G-code language (Ćwikła *et al.*, 2017).

(4) Before starting the printing process it is also important to check if the machine is calibrated (Steuben, Van Bossuyt and Turner, 2015) and having loaded enough material (Gibson *et al.*, 2014). If the FFF machine is not properly calibrated or runs out of material during the process it could result in process failures.

(5) FFF process is automatic, however, during the process, it is important to observe if it is going how it is supposed to, especially early in the process of first layers. Where some anomalies could be observed such as improper bonding to the build platform, or general visual defects (Mwema and Akinlabi, 2020).

(6) Once the FFF process is complete, the part needs to be removed from the build platform (Gibson *et al.*, 2014). Additionally, the build platform might require cleaning, especially if adhesives were used (Mwema and Akinlabi, 2020).

(7) After the object is removed from the build platform the parts might require some post-processing before they can be used for the designed purpose (Gibson *et al.*, 2014). Where the methods and purpose of post-processing were mentioned in section 2.2.

(8) Once the part is removed and/or post-processed, it can be used for its application. The application might vary, such as used for assembling to a final product (Gibson *et al.*, 2014), it could also be an additional treatment to prepare the product for its final use (Leirmo and Martinsen, 2019b).

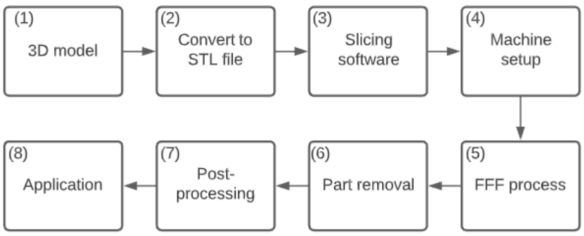

Figure 2.4: FFF process steps

2.2.2 Slicer software

A slicer is software that creates layers and the path of movement out of the STL file. The software has to consider features such as the geometry of the model to be printed, but also the physical features of the FFF machine. Knowing these features allows understanding what orientation the model needs to be printed in, but also if it requires any support structure. Additionally, in the software, you have the possibility to choose different machine parameters which will assure that the product will meet your needs (Horvath and Cameron, 2015). The choice of configurable parameters varies depending on the slicer software used (Kabir, S. M. F., Mathur, K. and Seyam, A.-F. M., 2020). Many different slicing softwares work on most FFF machines such as PrusaSlicer, Simplify3D, Cura, etc (Mwema and Akinlabi, 2020). Additionally, there is some proprietary slicing software such as Eiger for Markforged(Galati and Minetola, 2019). Once everything is prepared in the slicer software, it is possible to generate a code of the path and chosen machine parameters that a FFF machine will understand, most commonly G-code (Horvath and Cameron, 2015).

2.2.3 G-code

G-code is a programming language that was initially designed to control machine tools with the use of a computer. Although it is considered an old language from the 1950s, it still brings the benefit of using minimal computational power. This type of code is read in a sequence one by one. This means if a FFF machine receives a command, it performs the action that it is supposed to do and only once the first command is performed, then the next action is executed (Horvath and Cameron, 2015). Most FFF machines utilize RepRap G-code language, however, nowadays there exist many different types of FFF machine firmware’s, this results in some machine use different variations of G-codes (RepRap, 2021)

2.2.4 Process Parameters in FFF

Process parameters play a crucial role in achieving the desired quality out of the FFF process, either it is in form of mechanical strength, dimensional accuracy, or output speed. The process of selecting the right process parameters is by identifying the influence of each parameter and then deciding the best combination of the parameters. Mwema and Akinlabi (2020) Has classified process parameters into two categories, machine parameters, and material selection, as illustrated in Figure 2.5. Machine parameters are parameters that will decide how the object is going to be printed which are usually selected in slicing software. Whereas material selection is the process of selecting the right materials for the process.

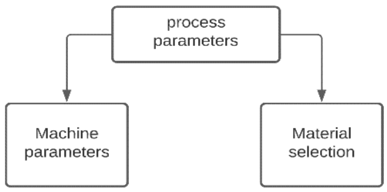

Figure 2.5: Process parameters in FFF

Machine Parameters:

- Raster width: Width of the raster, Figure 2.6 (Mohamed *et al.*, 2016).
- Raster angle: Is the direction the material is deposited on the build platform, as illustrated in Figure 2.6. Various raster angles could lead to different mechanical properties (Liu, Lei and Xing, 2019) and material flowability (Mwema and Akinlabi, 2020)

- Air gap: Is the gap between adjacent raster's, Figure 2.6(Mohamed *et al.*, 2016; Dey and Yodo, 2019)
- Contours: is the number of solid layers in the vertical direction, Figure 2.6 (Mohamed *et al.*, 2016)
- Contour width: Width of the contours (Rathee *et al.*, 2017)

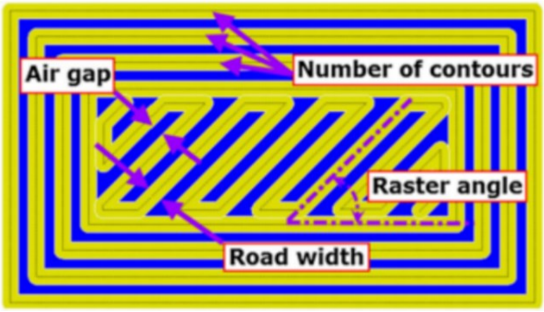

Figure 2.6: Illustration of raster width, raster angle, air gap, and number of contours (Mohamed *et al.*, 2016)

- Topp and bottom layers: Amount of solid horizontal layers on top and bottom of the object (Elkaseer, Schneider and Scholz, 2020).
- Build orientation: Describes at which angle and position the object will be printed in (Mwema and Akinlabi, 2020)
- Layer thickness: Also called layer height is the minimal height between layers, the variation could vary from several micrometers to millimeters, depending on machines capabilities and its application (Mwema and Akinlabi, 2020)
- Extrusion temperature: Is the hot end temperature where the semi-molten plastic is extruded (Mwema and Akinlabi, 2020).
- Build Platform temperature: Is the temperature on the build platform, it improves the adhesion properties of the plastic to the build platform. If the plastic doesn't adhere to the bed correctly, it can influence dimensional accuracy and lead to failures as the nozzle gradually blocks the flow of the extrusion. However, some FFF machines do not contain a heated build platform, in those cases, the use of adhesives such as glue could be an alternative (Mwema and Akinlabi, 2020)
- Printing speed: Is the speed of the print head and build platform (Domingo-Espin *et al.*, 2018).
- Travel speed: Speed of print head during non-printing (Ultimaker, 2020b).
- Feed rate: In G-code travel and printing speed are described by one parameter, which is Feed rate (RepRap, 2021).
- Extrusion speed: Extrusion speed determines the speed of the extrusion, where the amount of extrusion speed results in different material widths (Domingo-Espin *et al.*, 2018).
- Flow rate: Describes the amount of material being extruded (Tagami *et al.*, 2017).
- Infill pattern: Is the internal structure of the model Figure 2.7, there are various types of patterns that are used to optimize strength and durability (Dey and Yodo, 2019)
- Infill density: As the name suggests, it is the density of the internal structure, which greatly influences the resulting mass and strength of the printed object (Dey and Yodo, 2019).

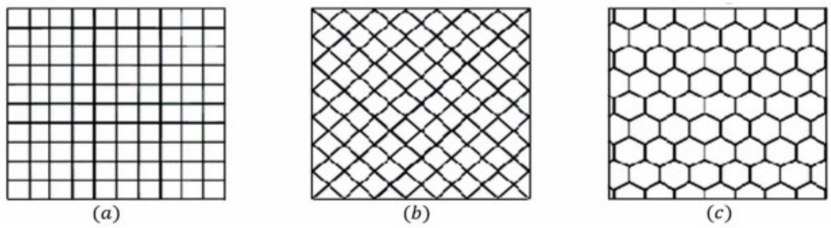

Figure 2.7: Examples of different infill patterns (a) linear, (b) diamond, (c) hexagonal (Dey and Yodo, 2019)

- Retraction: Process of retracting filament during non-printing states, such as movements between surfaces or while it is paused. Retraction parameter consists of retraction speed and length. When the material is retracted it reduces pressure inside the nozzle and minimizes material leakage (Greeff and Schilling, 2018)
- Z-offset: Is the distance between nozzle and build platform (Shembekar *et al.*, 2018).
- Jerk: Is the maximum instantaneous speed change of print head (Bui, 2019)

Additionally, some of these parameters could be subdivided into smaller categories of parameters, which specify parameters for specific states. Such as printing speed for contours, infill, first and top layers, etc. (Mendricky and Fris, 2020; Elkaseer, Schneider and Scholz, 2020).

Material selection

When looking at the materials, the determining factor for the glass transitioning temperature of the material is the chemical properties, but also printed parts quality. Thermal properties affect the melting point and flow through the nozzle and melting conditions. Mechanical properties are the determining parameter for the rigidity of the printed part, depending on mechanical properties it can also result in a clogged nozzle, due to strength and friction from the material in a semi-molten state (Mwema and Akinlabi, 2020). Moreover, it is also noted by Mwema and Akinlabi (2020) that information of material properties by filament brands might be inaccurate and therefore is recommended doing own testing of the properties to be sure.

2.2.5 Materials in FFF

Materials in FFF could be classified into three classes; single, composites, and blends. Single materials are polymer materials that are not mixed with other materials. Acrylonitrile butadiene styrene (ABS) is one of the most widely used polymers in FFF, provides great chemical resistance, toughness, and dimensional accuracy (Garcia *et al.*, 2010). Whereas polylactic acid (PLA) is the second most used polymer in FFF (Peterson, 2019), due to its low cost, low process temperature, however, it contains low crystallization which results in poor mechanical properties (Harris *et al.*, 2019). Poly carbonate (PC) is another material that contains great mechanical, properties, which are even better than ABS. However, it is a considerably more difficult material to process, which is also sensitive to moisture and can lead to brittle processed products (Peterson, 2019). Nylon is a flexible material that contains good mechanical and chemical properties, however, just like PC, it absorbs moisture (Harris *et al.*, 2019). Additionally, there are many more single materials that are available in FFF, such as High impact polystyrene (HIPS), polyurethane (TPU), polyethylene terephthalate (PET), polyethylene terephthalate glycol (PETG) (Harris *et al.*, 2019; Peterson, 2019).

However, these are commercial polymers, there are also non-commercial such as polyether ether ketone (PEEK). PEEK can provide superior mechanical properties compared to alternative FFF materials. Nevertheless, it is one of the most complicated materials to process, due to the need for high and narrow ranges of temperature (Harris *et al.*, 2019).

Composites introduce the possibility to manufacture parts that contain significantly more strength than just pure single materials. Which can provide better mechanical, conductive, and thermal properties. Where the composites could be either in form of synthetic such as fibers of carbon, kevlar, glass, metal, etc. It could also be in form of natural such as fibers of hemp, jute, wood, etc. Composites are also split into two categories, continuous and discontinuous. Continuous reinforcement is being deposited directly on top of polymer during the process to attain impregnation. Whereas discontinuous are powder or nanotubes of fibers that are short, micro, or nano, which are mixed with polymer (Harris *et al.*, 2019). One of the studied machines is Markforged Mark two, it processes both continuous and discontinuous composite materials. Where the discontinuous material Onyx is nylon with chopped carbon fibers, where the fiber volume is approximately 15-20% (Tantillo, 2019).

Blends are another type of material class, which consists of blending different polymer materials. As mentioned in the section 2.2 that FFF introduces anisotropic structure, however, studies show that blend materials could potentially minimize or even eliminate anisotropy (Spreeman, Stretz and Dadmun, 2019). Where the goal is to blend printable materials with non-printable materials. Some examples of blend materials are polylactic acid graft maleic anhydride (PLA-g-MA), styrene-ethylene butylene styrene (SEBS), styrene-maleic anhydride copolymer (SMA), etc (Harris *et al.*, 2019).

2.2.6 Process failures in FFF

In FFF there is a wide range of process failures that can occur during the process. These failures can occur due to incorrect process parameters, material choice, mechanical and electrical components. In this study, a process failure is considered something that occurs during the process without consideration of failures due to solely caused by mechanical component wear.

Material runout

Material runout is type of process failure which leads to machine running out of the material. This would result in that the processed object is not finished and since it is a single step process, it would be required to be started over again [12].

Ghosting

Ghosting is type of process failure that produces visual artifacts in form of waves on surface of the model. Ghosting occurs primarily due to excessive vibration on FFF machine, which could come from the rapid movements of the print head and build platform. However, if the vibration is large enough it could lead to complete failure of the printed model (Duan, Yoon and Okwudire, 2018). In form of process paramters, feed rate has strong influence on vibration of the machine (Li, Y. *et al.*, 2019).

Warping

Warping is a type of adhesion failure which causes corners of the printed object's base to lift, as illustrated in Figure 2.8. This type of failure introduces dimensional errors, structural defects, pores, and cracks on the processed object (Mwema and Akinlabi, 2020). Warping occurs mainly due to material shrinkage during the process. During the extrusion process, material expands, but once it starts to cool down it starts to shrink. If the shrinkage is too large, the corners of the printed object bend and lift from the build platform. Warping is affected by several causes, such as material properties, adhesion to the build platform, print parameters (Ultimaker, 2020d), and ambient temperature (Khan *et al.*, 2020). Material properties affect in form of having different shrinkage properties than others, which could result in some materials warping more than others. Adhesion to the build platform is critical as without proper adhesion object might warp or become completely loose from the build platform. To achieve proper adhesion, it is critical to have the build platform calibrated.

Additionally, having an enclosure or a heated build platform is recommended, alternatively use of adhesives. Looking at print parameters, the use of a raft of brim could be required to achieve proper adhesion, which is some additional layers around the printed object to keep it more rigid to the build platform. The first layers of the process are critical in terms of warping failure. Therefore, choosing the right initial layer speed and layer height could greatly influence the adhesion. Lowering the initial speed would allow material to adhere properly and increasing first layer height results in calibration of the build platform to have be not as critical (Ultimaker, 2020d).

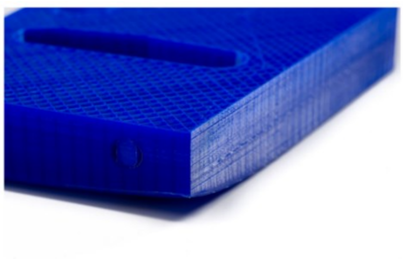

Figure 2.8: Illustration of warping in corners (Ultimaker, 2020d)

Pillowing

Pillowing is a type of failure which creates holes and bumps in the printed object, as illustrated in Figure 2.9. This type of failure occurs due to print parameters such as not having enough horizontal layers, or inadequate cooling during the process. Where the choice of horizontal layers depends on the layer height, the lower layer height the more horizontal layers are needed (Ultimaker, 2020a).

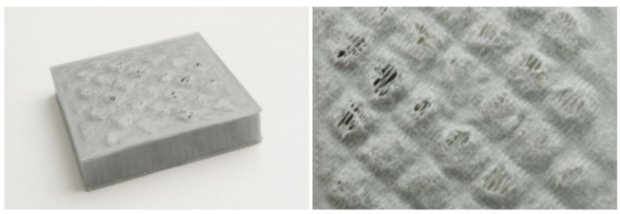

Figure 2.9: Pillowing defect (Ultimaker, 2020a)

Sagging

Sagging is a type of failure occurs during printing of complex geometries which have some form of overhangs. Where the cause of this failure is mainly due to parameters such as material properties, insufficient cooling, extrusion temperatures, and layer thickness (Kuznetsov *et al.*, 2019). Commonly, an additional support structure is required when an object contains angles above 45° (Hsiang Loh *et al.*, 2020).

Over and Under-extrusion

Under-extrusion is a type of failure which is caused by restricted material flow, whereas over-extrusion is caused by excessive material flow (Ultimaker, 2020c; Jin, Zhang and Gu, 2019). The result of under-extrusion would be rough surface, thin and incomplete layers. While for over-extrusion it would be excessive material on the object, containing a rough surface. Both types of failures could potentially lead to total failure of the printed object (Ultimaker, 2020c; Mwema and Akinlabi, 2020). Figure 2.10 illustrates good printing quality, over and under-extrusion. This type of failure is more challenging to solve due to the causes might be many things. It could be the print parameters are not set according to the material choice, or machine is not properly calibrated.

In terms of machine parameters, flow rate has a direct impact on the amount of material flow, as mentioned in section 2.2.4 about process parameters. Additionally, a combination of parameters such as print speed, layer height, and hot end temperature is strongly dependent on the amount of flow that is possible through the nozzle. If the layer height and print speed are increased while the temperature is maintained the same, it might cause under-extrusion, due to the amount of material being extruded. Furthermore, the nozzle diameter size has an influence on over and under-extrusion (Ultimaker, 2020c).

Looking at the mechanical parts of the machine, feeder of the filament might not be properly calibrated, where the tension on the idler might be too lose or too tight. Which would result in not enough material moving to the nozzle or grinding of material respectively. Additionally, grinding of filament could introduce other problems such as particles of grinded material ends up in the bowden tube where the material is fed. Where the particles in tube could create friction and restrict the flow of the material to the hot-end(Ultimaker, 2020c). Moreover, other possible causes are entangled filament or moisture in filament (Ultimaker, 2020c).

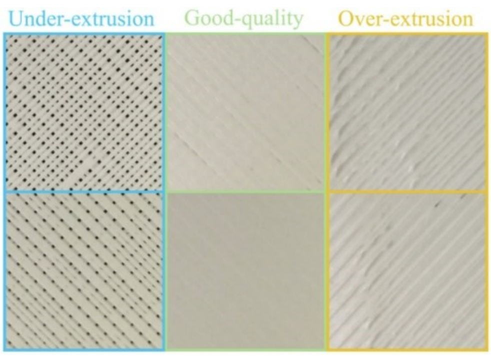

Figure 2.10: Illustration of good quality, under and over-extrusion (Jin, Zhang and Gu, 2019)

Stringing

Stringing also called oozing (Shaqour *et al.*, 2021; Baş, Elevli and Yapıcı, 2019) is a type of failure that results in the model containing thin plastic strings (Khan *et al.*, 2020), which causes poor surface roughness, as illustrated in Figure 2.11. This type of failure is impacted by material properties and machine parameters. Looking at machine parameters, there are mainly three main critical parameters that cause this type of failure. It is retraction settings (Ultimaker, 2020e; Greeff and Schilling, 2018), hot end temperature, print, and travel speed. When the print head moves between surfaces, material has to be retracted through the movement to avoid material leakage from the nozzle. Having the proper hot end temperature results in the right material consistency, if hot end temperature is too high for the material it could also cause material leakage. Finally, speed of the printing process and travel movements should be set accordingly, as slow speeds might build up too much plastic from both movements between surfaces, but also while printing. However, print speed and hot end temperature have to be set accordingly, otherwise, if the temperature is too low and speed is too high, it could potentially cause under-extrusion (Ultimaker, 2020e). Where in terms of material properties, poor quality of filament could introduce stringing (Hsiang Loh *et al.*, 2020).

Figure 2.11: Illustration of stringing (Ultimaker, 2020e)

Clogged nozzle:

A clogged nozzle is when material builds up in the nozzle. Sign of clogged nozzle is primarily restricted extrusion flow, which is commonly caused due to incorrect extrusion temperature settings (Hsiang Loh *et al.*, 2020). This type of failure is a significant process failure, this is because it affects the quality of produced objects in form of dimensional accuracy, surface roughness, and mechanical properties. Additionally, it could be caused by collection of dust inside hot end, nozzle being too close to the printed object which could happen due to a warped object restricting the flow of the nozzle (Tlegenov, Hong and Lu, 2018). Additionally, nozzle clogging is more common during the extrusion of discontinuous materials with fiber, where the density of the fiber influences the cause of clogging (Croom *et al.*, 2021).

Extruder jams

Extruder jams are when filament does not flow properly from the feeder to the hot end. This is commonly caused by variation in filament diameters, which could potentially break or coil up the filament in the extruder. The result of extruder jams restricts the extrusion process which could cause under-extrusion (Ultimaker, 2020c) or damaging the extruder motor (Soriano Heras *et al.*, 2018).

Defects due to nozzle offset

If the nozzle is not properly calibrated according to the build platform, it could print too close or too far from the build platform. If the nozzle is too close it could result in damaging the layers. Whereas if the nozzle is too far, it could result in material cooling down before it has properly bonded with adjacent layers, which would affect the mechanical properties of the object (Khan *et al.*, 2020).

Curling and rough corners

Curled and rough corners commonly occur due to extrusion temperature being set too high for the material which causes it to curl as illustrated in Figure 2.12 (Baş, Elevli and Yapıcı, 2019). This is due to the material not having enough time to properly cool down, which is also influenced by the fan speed (Hsiang Loh *et al.*, 2020)

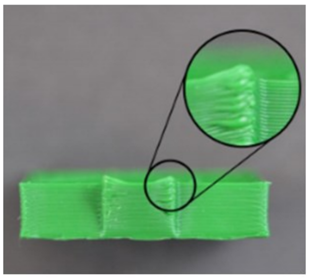

Figure 2.12: Curled edges (Baş, Elevli and Yapıcı, 2019)

Layer defects

During the FFF process, there are some common layered defects could occur. Figure 2.13 (a) illustrates missed layers, which commonly occur due to signs of under extrusion, too high printing speed, or mechanical issues with the Z-axis (Baş, Elevli and Yapıcı, 2019). Separated layers, Figure 2.13 (b), are commonly caused due to low extrusion temperature which does not allow layers to bond properly. Additionally, layer height influences the bonding, it is recommended to use lower layer height than the diameter of the nozzle (Baş, Elevli and Yapıcı, 2019). Misalignments are when stepper motors are incorrectly performing movements due to lost steps (Moretti, Bianchi and Senin, 2020a) and causing misaligned layers, as illustrated in Figure 2.13 (c). This type of failure is commonly caused by fast printing or acceleration speed (SIMPLIFY3D, 2021). Moreover, other causes for misalignment could be electrical and mechanical, such as overheated extruder motors or not properly calibrated mechanical components of the machine (Baş, Elevli and Yapıcı, 2019).

Figure 2.13: Layer defects (a) missed layers (b) separated layers (c) misaligned layers (Baş, Elevli and Yapıcı, 2019)

2.3 Monitoring systems nowadays

With the advancement of technologies, the amount of data acquired has been significantly increasing (Syafrudin *et al.*, 2018). As the manufacturing processes become more complex nowadays, it results in additional process parameters and system conditions that are necessary to be monitored (Lu and Wang, 2019). Monitoring systems are being used for various applications such as, improving production, reduce expenses, predicting diseases, and warning systems (Syafrudin *et al.*, 2018). For monitoring of industrial machinery states, commonly condition monitoring is implemented, where the focus is on detecting failures as early as possible, in order to maximize productivity (Márquez *et al.*, 2012). Event monitoring is the process of detecting a certain occurrence of events (Lai *et al.*, 2018). In computing systems, system monitoring is commonly used to track the performance of the system and possible attacks (Gao *et al.*, 2018). Monitoring systems are mainly composed of a combination of data acquisition and data analytics. Where the data can be various things such as events, images, sensor data, process logs, etc (Syafrudin *et al.*, 2018).

As the focus of this study is failure detection during FFF manufacturing process, it will primarily be focused on condition monitoring (CM). Which is the process of detection of faults based on monitoring machine parameters and their deviation from targeted values. CM primary focus diagnosing, predicting machine health, and fault detection. CM could be categorized into three types, offline, online, and real-time. Offline CM is when data is acquired and analyzed at unspecific times. Online CM is when data acquistion happens with some specific time intervals, however, the analysis and corrective measures are not. Whereas, in real-time CM both data acquistion and corrective measures are done with some specific controlled intervals (Wong, Chuah and Yap, 2020).

Although implementing CM systems could be complex and costly, it provides the possibility of detecting gradual failures, rather than just sudden failures. In manufacturing sudden failures result in no way to detect the failure before it has occurred, therefore it is an unwanted behavior. Whereas, with CM it is possible to observe the gradual failures, which allow taking corrective measures (Wong, Chuah and Yap, 2020).

The process of acquiring internal data is not something new, it has been used in terms of tool CM in CNC milling. Just like FFF machines, CNC machines are also equipped with some sensors, they provide the possibility to detect some failures, without the need for the complexity of external sensors. However, it is also noted that internal sensors are limited with information that they can provide. This could be from various reasons, such as the sensor not capable of capturing the area of interest, which could be due to sensor placement being too distant from the process, which also affects the quality of the data (Wong, Chuah and Yap, 2020).

Therefore, in order to know if external sensors are required, it is important to understand what is being measured. If the internal sensors are not capable of capturing the process, there is a need for external sensors. Sensor placement plays a crucial role in the quality of the data acquisition, where the placement is figured out through trial and error or expert experiences (Wong, Chuah and Yap, 2020).

Additionally, the choice of the sensor also plays a major role in terms of cost and complexity of the system (Soman *et al.*, 2019). This is because choosing the right type of sensor might reduce or even eliminate noise factors that other sensors would have observed. An example was a study by Tlegenov, Hong and Lu (2018) which investigated FFF process failure nozzle clogging. Their study showed that it was possible to monitor nozzle clogging by observing vibrations of the FFF machine. This was because as the nozzle starts to get clogged, vibrations increased around the print head. However, their study noted also that additional noise vibrations can occur from the machine itself. This introduces complexity of separating between vibrations caused by clogging or external noise. Moreover, the Tlegenov, Lu and Hong (2019) investigated the same type of failure, nozzle clogging. But this time the choice was to observe nozzle clogging through changes in current. As the nozzle starts to clog, the extruder motors need to exert more torque, this introduces changes in currents of the motor. This resulted in monitoring of nozzle condition with less complexity as it was not susceptible to noise as monitoring by observing vibrations. Moreover, sensor durability has to be considered according to its environment, as some environments might be to harsh for some sensors (Ghosh *et al.*, 2019).

It is also important to consider that not all machine failures could be measured directly. Direct methods are capable of measuring wear or defects directly, where it could be in form of visual detection such as machine vision or optical microscopy that is applied. Commonly in CNC tool wear, these direct methods are challenging to apply on online monitoring or without stopping the process occasionally (Wong, Chuah and Yap, 2020). However, in terms of FFF this is not necessarily the case, as most of the described process failures introduce some form of visual defects on the processed part. Therefore it could be possible to implement direct online methods in form of a vision system, as it has been done by (Shen, Sun and Fu, 2019) in FFF. While indirect methods focus on acquiring the data of process parameters of interest. However, indirect methods are less accurate but are also easier to apply in an online CM (Wong, Chuah and Yap, 2020).

During the data acquisition, it is also important to consider what types of data to acquire. As collecting all types of data might not be relevant or practical in online and real-time systems. However, in some cases it might be needed to acquire large amounts of data, these systems introduce a need of data acquisition methods that are capable of handling large amounts of data (Di Paolo Emilio, 2013). This is because the more data collected it introduces need for better memory and processing power to have the ability to collect and process data with minimal delays (Sirojan, Phung and Ambikairajah, 2018). There are three types of data, static, dynamic, and intermediate. Static data is a form of constant, which maintains the same value over a period of time. Although acquiring static data does not change during the process, it has a significant role in identifying information about the process. Dynamic data is a type of data that changes during the process, such as describes process state. Where the dynamic data directly indicates the process state and quality. Lastly, intermediate data is the data which is computed based on static and dynamic data (Hu *et al.*, 2018).

Furthermore, data acquistion commonly requires a form of storage of the data (Syafrudin *et al.*, 2018). There are mainly two types databases relational and non-relational. Where the choice of database highly depend on type of data acquired. An example is a comparison between SQL which is relational and NoSQL which is non-relational databases. where one of the key differences is that SQL works with structured data, while NoSQL works with unstructured data (Sumalatha, Vookanti and Vannala, 2021). Additionally , other factors that could be of importance during the choice of a database is scalability, availability, and flexibility (Syafrudin *et al.*, 2018).

With the large amount of data gathered, it introduces complexity in analyzing the data. Machine learning (Syafrudin *et al.*, 2018) and Neural networks are some of the common processing methods that are applied in the field of monitoring (Wong, Chuah and Yap, 2020).

In terms of acquiring data from physical phenomena from external sensors, commonly it is used a data acquisition card to acquire and process data. The fundamental process flow aspect of data acquisition system is shown in Figure 2.14. Sensors provide the possibility to detect different physical conditions such as electrical signals, radiant energy, mechanical energy, magnetic energy, thermal energy, and movements. Their task is to convert the energies observed into electric signals. Where the type of sensor used is dependent on the type of physical condition that is of interest. When the data from the sensor is observed it is then sent into signal conditioning. Signal conditioning is the process of modifying or amplifying the signal that it meets the needs of the next system (Di Paolo Emilio, 2013). This could be done with numerous types of techniques such as voltage amplification, filtering, timekeeping, etc. (Todd, 2014). Once the signal is conditioned it is then converted from analog to digital form, which allows computer to understand the data. Finally, a computer is used to visualize, store, and analyze the data (Di Paolo Emilio, 2013).

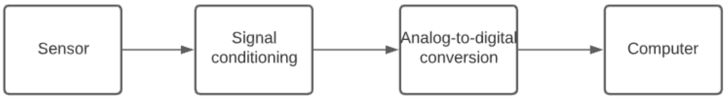

Figure 2.14: data acquisition system process flow

However, the machines are becoming more advanced with more integrated sensors which also have the ability to communicate over a network. This introduces the possibility of data acquisition over a network, without any external physical connectivity required. In addition to eliminating the need for a physical connection between the devices, data acquisition could reduce costs and increase efficiency (Hu *et al.*, 2018).

In data acquisition of manufacturing process, commonly data consist of primarily dynamic data, due to focus on observing the actual process. However, acquiring dynamic data introduces complexity, as machines are equipped with numerous sensors, but also commonly acquisition of data is of various types of machines. This is especially challenging as industrial machines commonly contain their proprietary communication and interface protocols. Additionally, the process of data acquisition becomes complex when different machine data are being acquired, especially if they contain different types of data (Hu *et al.*, 2018). As the data acquisition happens over a network, a communication layer is required. Communication standards such as OPC UA are specially designed for monitoring of industrial equipment, which also assesses the challenges with interoperability. MTConnect is another communication protocol that has been used in monitoring and data acquisition of machinery.

Moreover, the data acquisition methods keep evolving which provides easier access to the data. Data that is publicly available on the websites is possible to acquire through web scraping methods (Tao *et al.*, 2018). Whereas it is also becoming more common that machines are already equipped with sensors and some logic in form of a computer from the manufacturers. This results in the possibility for machine manufacturers to provide the ability to access the data of sensors directly, such as through application programming interfaces (API) (Xiao, Huang and Zhao, 2018).

2.3.1 REST API

API is a way two applications can communicate with each other based on a set of specifications and rules, most commonly communication happens over a network (Jacobson, Brail and Woods, 2012; Wu *et al.*, 2020). Essentially it provides a simple and reliable way to access data quickly between different parties such as between a provider and a consumer (Jacobson, Brail and Woods, 2012).

Generally, to access the data from APIs a code has to be written, and this can be a complex task (Alrashed *et al.*, 2020). However, some APIs are made to be accessible to the public by the providers (Maleshkova, Pedrinaci and Domingue, 2010) and their documentation (Jacobson, Brail and Woods, 2012). Public APIs bring the advantage of increased development by having them published to the consumers, without them needing to reinvent the wheel and rather focus on building on top of it. However, public APIs expose themselves to some risks such as attacks against information and APIs (Jacobson, Brail and Woods, 2012).

Representational State Transfer (REST) is a lightweight software architecture that is built on hypertext transfer protocol (HTTP) that provides interoperability over the internet for computer systems. Whereas REST API is an API that utilizes the REST architecture. REST API works as request-response communication, which allows to request systems to access and manipulate resources through HTTP methods in form of stateless operations (Chen *et al.*, 2017). Figure 2.15 illustrates the REST API communication between a client which requests and a server that responds to the request. The request methods could be different things such as modifying something (POST, PUT, DELETE) or requesting information back (GET) (Gao, Zhang and Sun, 2011). The response is commonly in a JavaScript object notation (JSON) data format (Bertoli *et al.*, 2021). REST API focuses more on Uniform Resource Identifier (URI) resources, which essentially means that each object has a unique URI identification that could be accessed directly (Gao, Zhang and Sun, 2011).

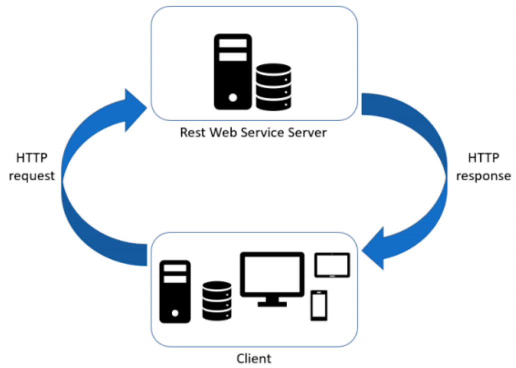

Figure 2.15 REST API communication (Bertoli *et al.*, 2021)

Commonly REST API contains a structured hierarchical manner of accessing the data relative to its origin path (Surwase, 2016). An example of Ultimaker API is illustrated in Table 2.2. Where firstly the "/printer" data various types of data of FFF machine. Whereas "/printer/bed" describes a more specific type of data which is the data of build platform. This type of structure allows accessing API data of specific resources directly, without the need for much processing.

Table 2.2 Ultimaker REST API structured path for accessing build platform temperature

Resource path	Description
/api/v1/printer	Different data available from FFF machine
/api/v1/printer/bed	FFF build platform data
/api/v1/printer/bed/temperature	FFF build platform temperature data
/api/v1/printer/bed/temperature/current	FFF build platform current temperature data

2.3.2 Web scraping

Nowadays with the increased connectivity, it has increased the amount of information out on the world wide web (WWW) also know as web (Chaulagain *et al.*, 2017). Although the web provides with possibility to access the data, there is no direct functionality in form of storing the available data, especially if public web APIs are not available to directly access data. This results in the need of manually copying the data and storing it, which is nor practical or possible realistically possible with dynamic real-time data. Additionally, extracting the data is complex as most web pages are written in HTML format and in an unstructured manner. This resulted in development of tools such as web scraping, which are automated tools for extracting the data from the web. Web scraping is being used in a wide area of applications to store data from the web. Such as web research, data integration, monitoring weather data, price comparison (Singrodia, Mitra and Paul, 2019). However, it has also been used of monitoring sensor data through the web (Rao *et al.*, 2015). There are many different types of web scraping library tools such as Scrapy, BeatifulSoup, and Grab. Nevertheless, these types of libraries only work on static pages, which contain no dynamic data (Chaulagain *et al.*, 2017). In order to scrape dynamic data, web scraping tools such as Selenium is specially designed for these type of tasks (Ramya, Sindhura and Sagar, 2017).

Although web scraping comes with great possibilities of extracting data, it has several limitations. These limitations are primarily within availability in form of you are limited to acquiring data that is only displayed at the web. Additionally, you have no control over what happens on the web, if the website is not available to access, it results in no possibility of acquiring the data (Ghosh *et al.*, 2019). Additionally, if the web page changes the structure, it results in need of maintenance of the web scraping code (Gladen and Staudt, 2020). Nevertheless, although web scraping contains questionable reliability, studies show also that web scraping is an efficient tool in form of speed of acquisition. Which showed that it had possibility of acquiring data from the web faster than with use of API (Dongo *et al.*, 2020).

Selenium WebDriver

Web pages contain document object model (DOM), DOM ensures that web page elements are structured, in form of a node-like data structure (Brucker and Herzberg, 2018). Selenium WebDriver is a framework that uses locator strategies that are based on DOM. Figure 2.16 illustrates the Selenium WebDriver architecture. Scripts are a form of client that sends selenium commands in JSON Wire Protocol. Which is a REST API that uses JSON format messages over HTTP (Raghavendra, 2021). Where the scripts allow to control browsers and acquire data using different language bindings such as Python, Java, Ruby, etc (García *et al.*, 2020). Web driver works by identifying elements on a web page and executing actions such as acquiring the specific elements data on the real browser. Where in order to access the elements there is need for locators, which identify where the elements are located on the web page. Theese locators could be id, name, cascading style sheets (CSS), XML path language (XPath), etc (Patil and Temkar, 2017). Additionally, the web driver must be according to the type of browser, such as Chrome browser uses chromedriver, and Firefox uses geckodriver, etc. Where the communication between driver and browser is through HTTP protocol (García *et al.*, 2020).

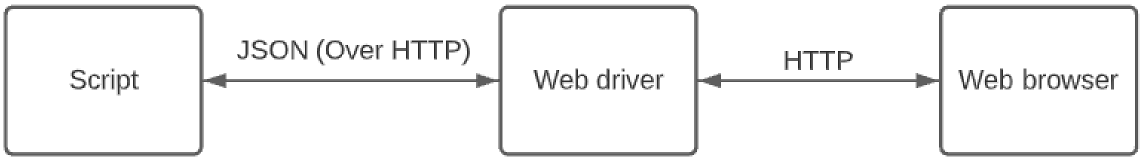

Figure 2.16 Selenium WebDriver architecture

3 Methodology

In this section it will firstly be presented the related stakeholders and how this thesis is related to their goals. Additionally, applied research methods such as literature review and experimental work will be described in detail.

3.1 Related stakeholders

This study is conducted in collaboration with Centre for Research-based Innovation (SFI) manufacturing and Manufacturing Technology Norwegian Catapult Centre (MTNC). One of the research areas of SFI manufacturing is robust and flexible automation, where in-process monitoring and real-time control is one of the focused topics. This study relates to the monitoring aspect of their research area in terms of that the primary objective in this study is to develop a data acquisition system.

MTNC plans to include additive manufacturing in the form of desktop FFF machines in a flexible production line, coordinated with other processes with the possibility of automation, robot handling of printed parts, and in-line quality control. Where the thesis provides the first steps towards their goal in form of the ability to acquire data of the FFF machines of their interest (Markforged Mark Two and Ultimaker 3 Extended).

3.2 Research methods

This research consists of both practical activities in form of experimental work and a literature review. Figure 3.1 illustrates the process of answering RQs, where all of them contained a mix of literature study and practical activities. In order to answer RQ1, it was investigated what types of data exist in FFF machines, which was primarily based on literature but also experimental work to confirm the available data. Based on RQ1 it was possible to explore RQ2 on what data is possible to acquire and how it could be acquired. Where literature provided with possible methods to acquire the data. Whereas experimental work was to establish data acquisition, which identified types of possible data to acquire. Additionally, it was investigated the possibility of generalizing data acquisition for studied FFF machines. Finally, RQ3 aimed at comparing the studied FFF machines in form of data quality through experimental work. Where data analysis was performed of the acquired data and compared to the literature if any of the described failures could potentially be identified with internal FFF machine data.

To conduct the experimental work, some activities are included in this study. These consist of creating a data acquisition system, FFF printing, data gathering, measurements of dimensional accuracy, and analysis of the acquired data. Whereas a literature review was performed both in order to support that the studied field is a relevant research topic, but also to support choices for experimental work.

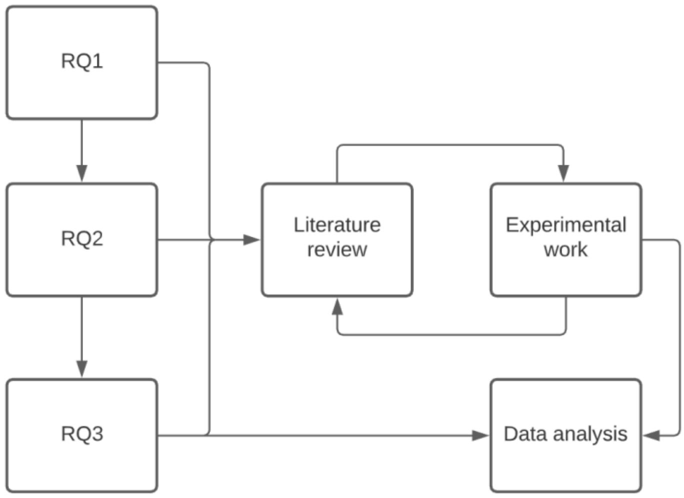

Figure 3.1: Process of answering research questions

3.3 Litterature review

In order to establish a solid background of the studied topic, it was first searched about generic about AM, on what it is, different types of AM technologies, and their key advantages and disadvantages. Keywords used were "Additive manufacturing", "Additive manufacturing technologies", "Advantages and disadvantages of different AM technologies".

Since this study is focused on FFF, which is a type of AM, it was research in more detail about it. Where the goal was to identify how FFF works and what is the process of FFF, which provided knowledge for experimental work. Here the keywords searched were "Fused filament fabrication", "Fused Deposition Modeling", "3D printing", "FFF printing process".

Once the fundamentals of FFF were identified it was then possible to look into what influences the FFF process in form of the most critical process parameters and type of failures that occur during the FFF process. These provide with knowledge about important data for RQ1 and the types of failures that occur for RQ3. Where keywords searched was "FFF process parameters", "FFF process failures"

Lastly, it was searched for what type of monitoring systems there are nowadays and how they work. This is to support the choices for RQ2 as this study is focused on real-time data acquisition of FFF machines. Additionally, it was also searched what are the challenges with such systems. Where the keywords used were "Monitoring systems", "Monitoring system challenges, "Real-time data acquisition systems".

3.4 Experimental work

Experimental work consists of four separate activities, where Table 3.1 provides a description of the hardware and software used for each activity. First experiment is focused on creating a data acquisition system for all studied FFF machines. As in order to understand if internal data could identify some failure in the FFF process, there is a need for data. The second experiment consist of FFF printing and data collection, this is for establishing a connection between an object and data. Based on printed objects, measurements were performed on a coordinate measuring machine (CMM). This is to compare the studied FFF machines and see if the collected data could potentially identify some anomalies during FFF process. Lastly, data analysis is performed in order to investigate the quality of the acquired data.

Table 3.1: Experimental work setup

Activity	Hardware	Software
FFF Printing	Original Prusa i3 MK3S	PrusaSlicer
	Ultimaker 3 Extended	Ultimaker Cura
	Markforged Mark Two	Eiger
Measurements	ZEISS DuraMax	Calypso
		PiWeb
Data acquisition	Computer	Python
		Chromedriver
		Chrome browser
	Raspberry Pi	OctoPrint
Data analysis	Computer	Python (Jupyter notebook)

3.4.1 Creating a data acquisition system

Since this study was based on already existing systems to access the data. This resulted in the need of investigating what are the existing systems for each FFF machine and if there is a need for additional components to access data. Based on that it was found that some FFF machines contained several methods of acquiring the data. Where the process of acquiring the data was chosen based on the literature on which was a more reliable method. The amount of data availability depended on the machine, such as Markforged Mark Two contained little access to the data, while Original Prusa i3 MK3S and Ultimaker 3 Extended contained considerably more. However, not all the data was chosen to acquire. Where the choice of the acquired data based on data that could describe process either in form of identifying the cause of failure or data which provided a possibility to identify when an event occurred. Additionally, the data was stored in a time-series format which is essential in order to have the ability to identify when a certain occurrence happened chronologically (Fu, 2011).

The code for data acquisition was generated in Python 3 programming language. A GitHub repository was created in order to share the code used in this study: https://github.com/KlaudijusN/Klaud_thesis.git. In addition, this repository contains raw data from this study experiments and code of other activities such as data analysis of printing and CMM data. For the data acquisition Python libraries included were (requests, json, time, sqlite3, datetime, selenium, and webdriver_manager). Where it was both acquired and stored data in SQLite database format. As the focus is on creating a real-time data acquisition, therefore the choice was SQLite as it is being used widely for various applications because it is a lightweight database system (Wang *et al.*, 2019). Additionally, the code went through iterations of testing and refurbishment to minimize the need for post-processing of the data for data analysis.

Finally, delays of the data acquisition were investigated. This is because the time of acquiring the data plays a significant role in form of data quality when looking at real-time data acquisition systems. Delays were investigated in form of comparing the data acquisition time for each FFF machine. Figure 3.2 illustrates the process of investigating acquisition delay. The data acquisition code was using a “while loop” in Python, which is a code to be executed repeated times. This repeated execution is the process of acquiring and storing FFF machine data for that specific moment. Whereas the acquisition delays were calculated based on the amount of time the while loop statement took to be executed. Where the difference in time of acquisition are delays. Additionally, the acquisition delays were investigated with the use of two different python time counters, which were “time” and “perf_counter”. As to develop real-time systems the data quality in form of data acquisition delays should be minimal. If the data acquisition process contains too high delays, it might result in no longer being real-time data acquisition as it is not capable of capturing the actual process.

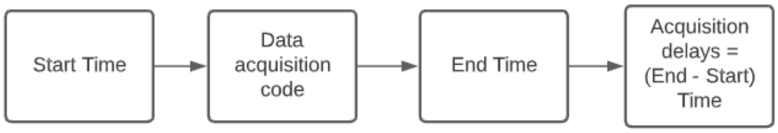

Figure 3.2 Process of investigating acquisition delays

Moreover, the type of computer has the potential to impact the quality of data acquisition, as it requires processing power to run the code. Table 3.2 provides a description of the computer and its main components.

Table 3.2 Computer used for data acquisition.

Computer	Microsoft Surface Pro 6
Processor	Intel Core i5 8250U (1.6 GHz)
RAM	8 GB

3.4.2 FFF printing and data acquisition

In order to investigate the quality of the data and compare between FFF machines if the data could provide some value in form of identifying some process failure, it was performed experimental FFF printing of an object. During the FFF process, it was used the created data acquisition to collect the data. FFF machines were located in different locations. Where Markforged and Ultimaker were at MTNC premises and Prusa at the author's home. Model for printing and CMM measurement path were acquired from the author of (Leirmo and Semeniuta, 2021) which was used in a study about dimensional accuracy of laser-based powder bed fusion AM technology. Figure 3.3 illustrates the printed object.

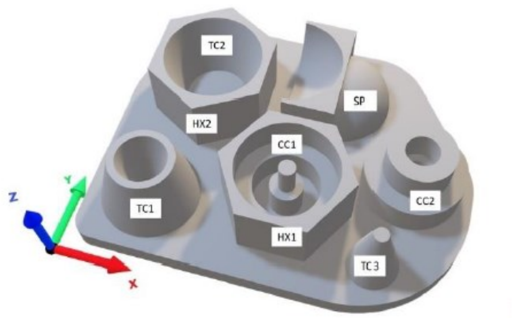

Figure 3.3 Experimental object (Leirmo and Semeniuta, 2021)

All the studied machines are not new and have been used, and since FFF machines contain many mechanical components, calibration and maintenance are necessary. Therefore, it is also important to state the author's experience with the studied machines, as although the process of FFF machines is the same. The way machines are built differently and result in different ways to calibrate and maintain them. Table 3.3 describes the authors experience with machines based on levels, where level 3 is the most knowledge and 1 is the lowest.

Table 3.3 Authors FFF machine knowledge level

FFF machine	Knowledge level
Original Prusa i3 MK3S	3
Markforged Mark Two	2
Ultimaker 3 Extended	1

Additionally, Markforged and Ultimaker have two extruders that can deposit material. However, Markforged has dedicated one for polymer material and a second one for fiber material. While Ultimaker has two extruders where any of its available materials can be printed from both extruders, where the choice of the extruder for experimental work was based on which had been least used. Table 3.4 provides an additional description of each machine, such as material type and brand, estimated process time, nozzle size, filament diameter, and more.

Table 3.4 Additional description of parameters used in the experimental printing

	Original Prusa i3 MK3S	Ultimaker 3 Extended	Markforged Mark Two
Nozzle size	0.4mm	0.4mm	0.4mm
Filament diamter	1.75mm	2.85mm	1.75mm
Material (brand)	PLA (PrintWithSmile)	PLA (3DNet)	Onyx (Markforged)
Material density	1.24 g/cm^3 (Abdullah *et al.*, 2019)	1.24 g/cm^3 (Abdullah *et al.*, 2019)	1.2 g/cm^3 (Markforged, 2020e)
Estimated process time	2 hours 51 minutes	2 hours 31 minutes	3 hours 2 minutes

Filament placement	Open	Open	Dry box
Machine enclosure	Open	Open	Fully enclosed
Class	Consumer	Prosumer	Industrial

Figure 3.4 illustrates the process flow of FFF printing and data acquisition. Before the experimental work of printing, each machine went through a testing phase, where it was printed some test objects to observe the current machine states. If some critical printing anomalies were detected, the machine went through a calibration phase. Which included things such as leveling the build platform and adjusting the distance between nozzle and build platform. Additionally, since Markforged does not contain a heated build platform, it was chosen to use adhesives for each printing process, as recommended by Markforged (Markforged, 2020d).

After machines were calibrated, it was then G-code was generated in slicing software with selected process parameters. In order to minimize variation and make the process most identical for all machines. Slicer settings were set to be most identical as possible, however, as mentioned in section 2.2.2 that on a slicer software available settings vary for each software.

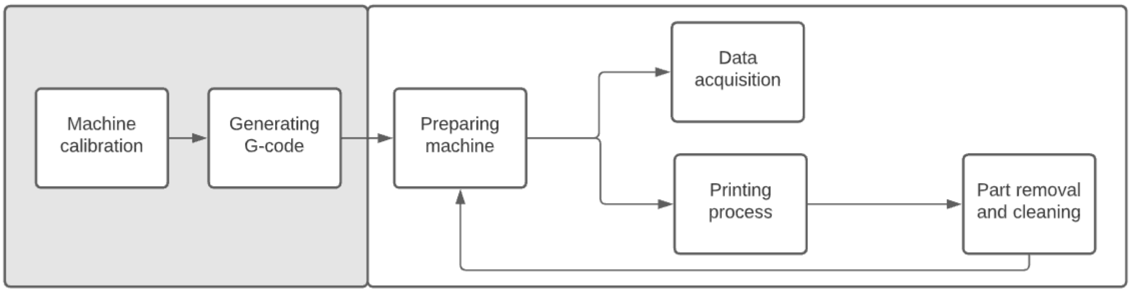

Figure 3.4: Process flow of FFF printing and data acquisition

Slicer parameters were selected to be as identical as possible for each machine. However, Markforged was limited with relatively few process parameters that were possible to select, Table 3.5 provides a description of selected process parameters for each Machine. Additionally, each slicer software contains somewhat different options for the same parameters, such as infill type and seam position. Where the options were chosen to be the most similar for each machine. Nevertheless, differences in how machines are built, some process parameters were not changed. As mentioned in section 2.2, the differences between Prusa having direct-extrusion, while Ultimaker having bowden-extrusion. Therefore, parameters such as retraction length and speed were the recommended settings from the slicer for Prusa and Ultimaker. Fan speed was selected to be standard for Prusa and Ultimaker, which were 100% fan speed except for the first 5 layers. Where the first layer starts at 0% and increases by 33% for every layer until reaching maximum fan speed.

Table 3.5: Selected process parameters for the printing process.

Parameters	Original Prusa i3 MK3S	Ultimaker 3 Extended	Markforged Mark Two
Hot end temperature	200°C	200°C	275°C

Build platform temperature	60°C	60°C	
Infill type	Rectilinear	Grid	Rectangular
Infill density	15%	15%	15%
Contours	3	3	3
Top layers	3	3	3
Bottom layers	3	3	3
Layer thickness	0.2mm	0.2mm	0.2mm
Contour width	0.4mm	0.4mm	N/A
Raster width	0.4mm	0.4mm	N/A
Raster angle	[45, 135]	[45, 135]	N/A
Seam Position	Aligned	Sharpest corner	N/A
Fan speed	100%*	100%*	N/A
Flow rate	100%	100%	N/A
Travel speed	180mm/s	180mm/s	N/A
Initial layer speed	20mm/s	20mm/s	N/A
Top layer speed	50mm/s	50mm/s	N/A
Bottom layer speed	50mm/s	50mm/s	N/A
Infill speed	70mm/s	70mm/s	N/A
External contour speed	30mm/s	30mm/s	N/A
Internal contour speed	60mm/s	60mm/s	N/A
Acceleration	1000mm/s^2	1000mm/s^2	N/A
Contour acceleration	800 mm/s^2	800mm/s^2	N/A
External contour acceleration	N/A	400mm/s^2	N/A
Internal contour acceleration	N/A	800mm/s^2	N/A
Travel acceleration	N/A	5000mm/s^2	N/A
Jerk	8mm/s	8mm/s	N/A
Retraction length	0.8mm	6.5mm	N/A
Retraction speed	35mm/s	25mm/s	N/A

Before each printing process, it was inspected if the machine is cleaned and contains loaded material. While after each printing process, the build platform was cleaned and the objects were removed and stored in a box with dehumidifiers.

The data was collected only during the actual printing process, additionally, the computer was used for normal tasks during the process of data collection. Also, during the printing process, it was considered some of the FFF challenges, in form of not exposing the machine to external vibration and abnormal humidity and temperature. Moreover, during the printing process, the data was collected with a preset acquisition time of 1 second. Where the data of each FFF machine are stored in separate files.

3.4.3 Measurements of printed objects

Measuring of dimensional accuracy of the printed objects was done on a coordinate measuring machine (CMM), using a 3mm diameter tip stylus. The process of measurements was done in a combination of manual and automatic work. Firstly, the model was fixed to the fixture, which was also provided by the same author who created the object (Leirmo and Semeniuta, 2021). The printed parts did not contain any post-processing except around the base plate if there were some strings of left plastic, which could have hindered fixing model to the fixture. Then it was performed manual probing to identify the plane alignment, this is to assess the variation between objects. Figure 3.5 illustrates the manual probing, where (a) red dots represent manual probing points to identify the base plane which represents the Z-axis, and (b) represents points to identify the X and Y-axis. Once manual probing of identifying each axis is done, CMM turns into automatic mode, which performs measurements based on the generated path. For this study, only a few features were selected out to perform the measurements. Features measured were in form of geometric and dimensional characteristics. Where the selected features are roundness and diameter of CC1 and flatness of the base plate. Moreover, the measurements were performed three times on each object, this is in order to minimize the variation of the measurements. This included reinserting the part to the fixture for each measurement.

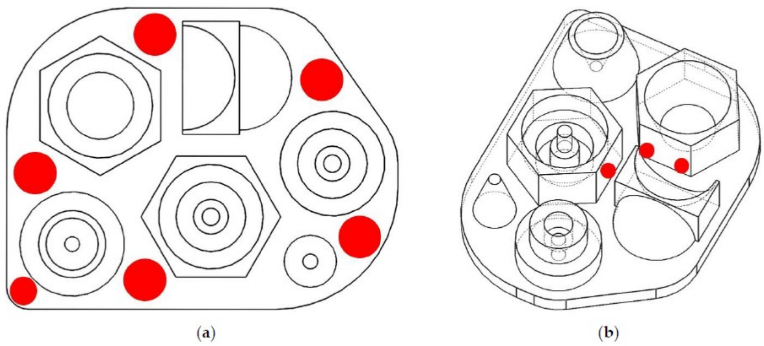

Figure 3.5: Manual probing points (a) Points for identifying Z-plane, (b) Points for identifying XY-plane (Leirmo and Semeniuta, 2021)

3.5 Data analysis

Data analysis was performed in Python Jupyter notebook. For the data analysis, Python libraries that were used were pandas, sqlite3, datetime, matplotlib, and seaborn. The steps involved in data analysis were structuring, cleaning, and visualization of the data. How the data analysis is performed plays a significant role on the results, therefore each data analysis step is described in the following subsections.

3.5.1 Structuring

In order to easily analyze the data, it has to be structured. This means that data should not contain nested data, which is data within data (Mertens, 2017). Therefore, the data should be in each separate row. Additionally, the data which will be used for analysis should be raw numbers without containing any text in them. Figure 3.6 illustrates an example of how the data was structured. However, as mentioned earlier in section 3.4.1 about the creation of data acquisition, that the code was generated in order to minimize post-processing of the data. Therefore, some of this process was already done in the process of creating the data acquisition for each machine.

(a)

	Layer	Fan_speed
0	1 of 105	-
1	2 of 105	33%
2	3 of 105	67%

(b)

	Current_layer	Total_layers	Fan_speed
0	1	105	0
1	2	105	33
2	3	105	67

Figure 3.6: Structuring (a) unstructured data, which contains nested and text data (b) structured data

3.5.2 Cleaning

In order to perform data analysis, the data has to be cleaned, which involves steps of removing invalid and unreliable data (Mertens, 2017). Here the invalid data represents data captured during the non-printing process.

Although the code was generated to capture when machine state is “Printing”, it was still observed that the data provided with some false positives. Since the focus is only on analyzing the actual printing process, it involved cleaning of data which were from other processes that were considered printing process, such as pre-heating, starting calibration, but also when the process stops. This is because machines during these processes might not have reached the target temperature and could potentially influence the rest of the data set. However, the types of data possible to acquire from each FFF machine and how the machine worked varied from machine to machine. The process of identifying when the machine actually started processing and ended varied.

In terms of unreliable data, it is a type of data that did not represent the actual process. During cleaning of unreliable data, it was looked into missing data and outliers. Where with the missing data it was investigated where that specific event occurred. It was then evaluated if that specific data variable would be used for further analysis. If the missing data of a specific variable was not used for further analysis, however, other variables for the same rows were used, which resulted in keeping the data rows. Additionally, it was investigated if those occurrences of missing data had some pattern of when it appeared.

Moreover, it was looked into outliers also called extreme values. However, due to the amount of data collected in the process, it was challenging to investigate each data point. Therefore, it was used descriptive statistics to investigate extreme values in form of maximum and minimum values. Where based on these values it was possible to identify if there were some anomalies in the data. Where the anomalies were looked into in more detail of why and when they happened. Based on that it was possible to choose if the anomaly was describing the actual event or it was an error in the data. The result of these allowed the choice of keeping or removing the data from the dataset.

3.5.3 Visualization

In order to provide a better understanding of the data, data visualization is performed, in form of a graphical illustration of the data. Additionally, it is provided with statistical description in cases visualization is not optimal. Visualization is essential to have the ability to interpret outliers and results, therefore it is performed during all stages of data analysis. Furthermore, visualization provides the readers with the ability to understand the causes and relationships of the analyzed data. Where the visualizing tools used are scatter, line, swarm, and bar plots.

4 Results

The result section is divided into three sections, where each corresponds to each RQ. Section 4.1 will be presenting the available data in FFF machines. Section 4.2 provides the methods used to acquire data from each machine. It will be described what data are possible to acquire from each machine based on the chosen methods. In addition, it will be presented the possibility of generalization of the data acquisition and challenges with it. Lastly, section 4.3 will be aiming at presenting the quality of acquiring data. Here will also the described failures be compared to the acquired data.

4.1 RQ1 Types of internal data in FFF machines

The internal data of FFF machines could be split into three categories, sensor, g-code, and firmware data. Sensor data is the type of data that is directly gathered from sensors. FFF machines are equipped with limited sensors. Table 4.1 describes sensors that are present in studied machines. Proximity sensor provides the possibility to identify the distance between the nozzle and build platform at different points. The result of measuring different points of the build platform could provide information of not just distance from the nozzle to the build platform, but also the build platforms alignment. IR sensors identify the presence of the filament, where an additional mechanical lever supplements the ability to detect filament and avoid errors (Research, 2021). Whereas thermistors are being used on every machine to identify temperature for aspects such as build platform, proximity sensors, electronics, but also each hot end temperature. Ambient temperature influences the accuracy of proximity sensors (Guo *et al.*, 2019). Ultimaker and Prusa contain proximity sensors, however, it was not found whether the proximity sensor on Ultimaker contains a thermistor. Nevertheless, Ultimaker may contain a thermistor for proximity, as during the printing process it performs calibration of measuring the distance from the nozzle to build platform only after machine has been heated. Limit switches are being used in machines to find its origin coordinates when starting a new process. Where Prusa uses specific stepper motor drivers, that allows sensorless homing of all axis (Prusa Research, 2021). Lastly, a camera that is able to capture video of the process.

Table 4.1: Types of sensors in studied FFF machines

<table>
<tr><th>Sensor</th><th>Description</th><th>Prusa</th><th>Ultimaker</th><th>Markforged</th></tr>
<tr><td>Proximity sensor</td><td>Measures the distance between the nozzle and build platform</td><td>X</td><td>X</td><td></td></tr>
<tr><td>IR sensor</td><td rowspan="2">Identifies the presence of a filament material</td><td rowspan="2">X</td><td></td><td></td></tr>
<tr><td>Mechanical lever</td><td></td><td></td></tr>
<tr><td>Hot-end thermistor</td><td>Measures the temperature of the nozzle</td><td>X</td><td>X</td><td>X</td></tr>
<tr><td>Build platform thermistor</td><td>Measures temperature of the build platform</td><td>X</td><td>X</td><td></td></tr>
</table>

Proximity thermistor	Measures temperature of proximity sensor	X	N/A	
Electronics thermistor	Measures ambient temperature around electronics	X	X	
Limit-switches	Detects XYZ-axis presence		X	X
Camera	Captures video of the process		X	

G-code data is the type of data that describes all the necessary details for the FFF machine to be capable of printing the object. It contains data in form of all the preset process parameters from the slicer software, additionally the different XYZ axis movements but also extrusion (E). It includes the different selected process parameters from the slicer software.

Although G-code is already available when it is generated from slicer software, it is very challenging to manually access the specifics of the data. There are some exceptions such as preset process parameters that could be accessed directly from the G-code and they are static values that do not change. However, data such as path movement, feed rate, fan speed, and layer height are all dynamic in the sense that they change depending on where in the print process machine is and/or what kind of geometry is being processed. Therefore, to understand when some failure occurs, it is needed to know where the machine was and what was the feed rate there.

Finally, there are firmware data that is stored internally in the FFF machine, which communicates with hardware devices. Where the type of data is print head position, but also firmware version and configuration.

In order to access these sensors, g-code and firmware data are needed for communication with the firmware. This is commonly done by implementing a computer or microcomputer which contains software that establishes the communication. Where the communication happens primarily through a terminal. When communication is established, the g-code data is being automatically published to the terminal as the code is being executed by the machine. Whereas in order to access the firmware and most sensor data, it is done by sending G-code commands to the FFF machine through the terminal. Table 4.2 provides some relevant data to access through G-codes.

Table 4.2: G-code commands for accessing data through terminal communication.

G-code	Description
M105	Reports current and target temperature of all thermistors
M73	Process progress
M114	Current print head position
M503	Reports firmware settings
M115	Reports firmware version

However, some G-code commands to access data are exclusively firmware specific, which results in some firmware's does not contain the possibility to access that data or G-code commands are different (RepRap, 2021). An example is retrieving proximity sensor data, Table 4.3 provides with Prusa-specific G-code, which requires a sequence of G-codes to retrieve data.

Table 4.3: Original Prusa i3 MK3S G-code for retrieving proximity sensor data.

G-code command	Description
G28 W	Homes XYZ-axis
G80 N7	Performs measurements on build platform in 7x7 grid
G81	Reports results of each measurement

Nevertheless, for Ultimaker and Markforged there was limited access to the machine, therefore it was not possible to physically acquire the firmware or G-code data. However, Ultimaker uses much of the same G-code commands (Cavdir, 2020) as by RepRap G-commons (RepRap, 2021). Which could mean if physical access to the machine was established, it could be possible to access the data. Whereas for Markforged it was not found any literature on how internal communication happens in the machine.

4.2 RQ2 Methods for acquiring data

4.2.1 Original Prusa i3 MK3S Data acquisition

Original Prusa i3 MK3S contains a motherboard (Prusa Research, 2021), which is primarily a controller board which is the logic behind the machine. It is the part of the machine that is responsible for transforming G-code into motion and temperature control (Carolo, 2021). However, it does not provide additional functionality such as accessing machine data. Therefore, in order to acquire the data from the machine, there is a need to establish communication with the machine. This was done by using a Raspberry Pi containing OctoPrint. Figure: 4.1 (a) illustrates the connection of Prusa to Raspberry Pi through a universal serial bus (USB), where a computer can access OctoPrint through WIFI. OctoPrint is an open-source application that provides a possibility to monitor and control FFF machines through a web interface (Needs *et al.*, 2019). In addition, OctoPrint contains plugins that provide additional functionality, in this case, additional data with the use of "DisplayLayerProgress" plugin (OllisGit, 2021). The selected data for data acquisition are described in Table 4.4.

The data acquisition was possible with both web scraping but also API's. The choice of data acquisition method was chosen based on section 2.3.2, the limitations of web scraping. Web scraping has a lot of dependencies such as the need for access to the web interface and that the information provided on the web can change. Although API also requires a server that provides access to APIs, its access to data maintains the same through unique resource identifiers (URI). These differences between API and web scraping resulted in the choice of API.

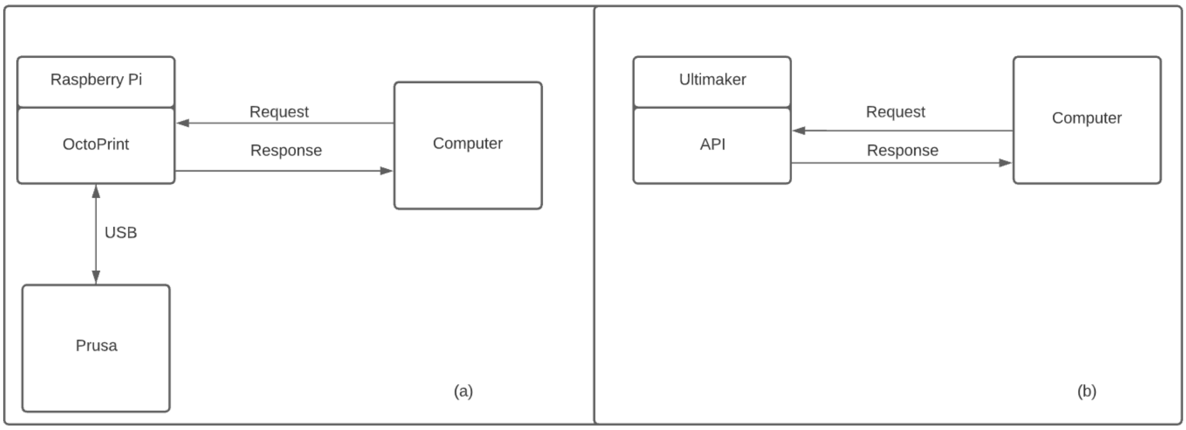

Figure: 4.1 Data acquisition with API (a) Prusa with OctoPrint API, (b) Ultimaker API

Table 4.4: Prusa API acquired data

Data	Description
Hot end temperature	Current temperature of the hot end
Hot end target temperature	Targeted temperature of the hot end
Build platform temperature	Current build platform temperature
Build platform target temperature	Targeted temperature of the build platform
Feed rate	Describes travel and printing speed
Machine state	Current state of the machine
Current layer	Current layer in the process
Total layers	Total amount of layers for printed object
Z coordinate	Current height of the print head
Object	Name of the processed object
Fan speed	Current fan speed in percentage
Process progress	Progress of the process in percentage
Process time	Time in process
User	User that initiated the printing process
Average layer duration	Average layer duration
Last layer duration	Amount of time it was used on previous layer

Moreover, it was not possible to acquire positional data, nor IR and proximity sensor data. When it comes to positional data, it is like mentioned in 4.1 that positional data is acquired by sending out G-code commands. In order to track the current position of the print head, it would require having constantly sending out the G-code. Where founder of OctoPrint stated that this would result in challenges as there is a limitation in communication between the FFF machine and Raspberry Pi due to USB-serial connection (Häußge, 2017). Additionally, for the IR sensor, it was not found any ways to acquire or access the data, nevertheless, it was observed that Prusa had integrated features with the IR sensor. Once the filament runs out, the process pauses until the filament has been changed, where it resumes from where it paused. Proximity sensor data was possible to acquire through terminal communication as described in results of 4.1, however, there was not found any existing method to acquire data from the terminal, nor was the author able to do it.

4.2.2 Ultimaker 3 Extended data acquisition

Unlike Prusa, Ultimaker 3 extended contains both a control board, but also an additional computer (Daid, 2016), which provides REST APIs (Ultimaker, 2021) and web interface monitoring (Kohut, 2020). Ultimaker is the only studied FFF machine that contains a camera sensor. Since most presented process failures could be identified visually, a camera sensor could be an important factor. Accessing camera video was only possible through the Ultimaker web interface, Appendix 1 illustrates camera perspective and quality during the process. However, it seemed like the camera contained low frames per second, which resulted in the choice of not focusing on acquiring camera stream. Additionally, unlike Prusa with OctoPrint, the web interface on Ultimaker is very limited on the type of data displayed. This resulted in a choice of API for data acquisition, where the connection is illustrated in Figure: 4.1 (b). Whereas Table 4.5 describes all the data gathered during the printing process. Additionally, as mentioned in 3.4.2, Ultimaker contains two hot ends that are possible to print out off, however, for this study we focused only on a single one. Where the choice of the hot end was the least used one, based on data from "hot end material extruded". Therefore, the data acquired was only for that specific hot end, however, it is possible to acquire data for both hot ends.

Table 4.5: Ultimaker API data

Data	Description
Machine state	Describes current machine state, such as if it is idle or printing.
Build platform temperature	Temperature of the build platform at current moment
Hot end temperature	Hot end temperature at current moment
Target temperature of build platform	The current targeted temperature of build platform
Target hot end temperature	The current target temperature of hot end
Position	XYZ-axis position
Fan speed	Current fan speed in percentage

Object	Name of the processed object
Process progress	Progress of the process in percentage
Head acceleration	Acceleration of the print head in XY-axis
Hot end material extruded	Amount of material extruded through the hot end in mm
Hot end time spent hot	Amount of time the hot end has been in a heated state
Hot end max temperature exposed	The maximum temperature hot end has been exposed to
Z-axis offset	Offset between build platform and hot end from manual calibration
Feeder jerk	Jerk settings of feeder
Feeder acceleration	Acceleration of feeder
Feeder max speed	Maximum speed of feeder

4.2.3 Markforged Mark Two data acquisition

Markforged Mark Two, just like Ultimaker contains also both a control board and a computer (Markforged, 2020b). These components provide with Eiger cloud software, which is a web-based slicer and user interface to monitor. However, Markforged machine and Eiger software is a very closed system (Aslanzadeh *et al.*, 2018; Korkees, Allenby and Dorrington, 2020), where communication with the machine is only through Eiger software. It was also not found any literature that investigated the potential of data acquisition of internal Markforged data. Additionally, it is not provided with any accessible APIs for the users, although API is being used for updating process state on Eiger web interface (Markforged, 2021). These limitations resulted in web scraping as a data acquisition method. Where Selenium WebDriver was the specific data acquisition method, due to the possibility of acquiring dynamic data from the web pages.

Moreover, Markforged G-code is not accessible due to encryption (Grimm, Pongratz and Ehrlich, 2020). This makes accessing specifics from the G-code such as preset process parameters but also additional information inaccessible. On Eiger, it is possible to access the history of printed objects, which contain information on what process parameters were selected when the model was sliced in slicer software. However, in Eiger slicer software there are only limited process parameters that that is possible to adjust. Therefore the data acquired from the print history would be limited (Kabir, S., Mathur, K. and Seyam, A.-F. M., 2020). Based on these restrictions, the choice of data acquisition method was web scraping, where the data access is limited to what is provided on the web interface.

Table 4.6 provides a description of the data collected. As mentioned in 3.4.2, that only one hot end was used for experimental work, which was polymer hot end. Therefore, data of fiber material such as type of material in use and temperature of the fiber hot end was not collected during the acquisition process.

Additionally, although the data acquisition is conducted only during the printing process, it was observed, during the development of the code and testing phase, that Markforged contains several different machine states. These machine states could have the potential in identifying a failure. Markforged is a closed system, it contains some features that can identify some process failures, such as fiber hot end jam (Markforged, 2020a). Once the jam is detected it was observed that the machine state identifies type of state, which was fiber jam. Additionally, if the data were collected during the non-printing process, it is also possible to capture other machine states such as when maintenance was performed.

Table 4.6: Markforged web scraping data

Data	Description
Polymer material	Current material polymer hot end
Polymer hot end temperature	Current temperature of the polymer hot end
Machine state	Current machine state
Current layer	Identifies in which layer the machine is processing currently
Total layers	Total amount of layers for printed object
Object	Name of the processed object
User	User that initiated the printing process
Time left	Estimated time left of process

4.2.4 Possibility of generalizing data acquisition of FFF machines

In order to generalize the results of data acquisition for all FFF machines, the machines must provide with the same type of possible methods to acquire data. Table 4.7, provides a description of possible data acquisition methods for each studied machine. Although Markforged, Ultimaker, and Prusa (with OctoPrint) provide with web-interface, the amount of data is limited compared to alternative methods for Prusa and especially for Ultimaker. Therefore, the result of generalizing the acquisition would impact the quality of the data in form of the type of data accessible and the reliability of the acquisition method. This would lead to sacrificing the quality of the data in order to generalize the data acquisition. Since the main goal of this study is to investigate if the internal data provides any value in failure detection. Therefore, the choice of the data acquisition method for Prusa and Ultimaker was based on the availability of the data, but also the more reliable data acquisition method.

Table 4.7: Possible data acquisition methods for each studied FFF machine

	Web scraping	API
Prusa	X	X
Ultimaker	X	X
Markforged	X	

4.3 RQ3 Quality of acquired data

The results of section 4.2 identified the possible methods for acquiring data and the types of data that were acquired. Appendix 2 lists all data that was used to acquire for each machine. In terms of failure detection all of the studied machines provided with a possibility to acquire hot end temperature data, in form of current temperature but also targeted. Although Markforged does not directly provide targeted temperature, it provides data in form of current material use which could be described as targeted temperature. Looking back at 2.2.6 about process failures. Types of failures that have the potential to be caused by hot end temperature are; stringing, sagging, curled edges, separated layers, over and under-extrusion. Whereas build platform temperature, which Ultimaker and Prusa provide, has the potential in identifying failures such as warping that is directly related to build platform temperature. While acceleration and feed rate have the potential of identifying failures related to speed. Which could have an impact on failures such as misalignments, missed layers, warping, stringing, over and under-extrusion. Data of fan speed provides the potential of identifying failures such as sagging, pillowing, and layer bonding. Nevertheless, it is important to note that failures have potential causes due to several variables as mentioned in section 2.2.6. Z-axis offset data has the potential in identifying offset values from manual calibration of the nozzle, which has an impact on failures related to defects caused by nozzle offset. Furthermore, observing data related to the feeder could identify issues related to stringing, as feeder is directly responsible for retraction parameters.

In terms of identifying where a specific event occurs in the process, various types of data could be used in detecting the event. Data such as current layer, total layer, XYZ coordinates, process progress, process time, process time left, machine state, hot end material extruded and time spent hot, average and last layer duration) provide with some form of identification of process.

Additionally, data that provide some statistics of the machines usage state, such as hot end state, in form of material extruded, time spent hot, maximum exposed temperature, could have an influence in terms of failure detection. Where material extruded could identify the failure of running out of material. Markforged and Ultimaker have no sensors to identify this failure. Although there has not been linked any direct potential failure caused by exposing hot end to extreme temperatures, there is still a certain limit to which components in the hot end could be exposed too. Exposure to higher temperatures could potentially cause some failures. Whereas the combination of these parameters and the amount of time hot end has been heated could identify the state of the hot end and thereby be a factor in terms of failures.

The following subsections will present the acquisition delays from the data acquisition of printed objects. Then it will be presented results of acquired data from each FFF machine. Lastly, the results of CMM measurements and their relation to the data will be presented.

4.3.1 Data acquisition delays

The data acquisition delays were investigated during the printing process of all objects for each machine. Acquisition delays are critical in terms of real-time monitoring systems, as it describes the minimal acquisition time interval possible to capture between different events. The influence of delays could also result in capturing data of process which does not correspond to actual process time. Considering real-time systems, it is therefore critical to have low acquisition delays, as it is needed to capture the actuall process. FFF printing is a continuous process with constant motion, therefore, it is important to capture data through the entire process with short intervals. Intervals for the acquisition were chosen to be 1 second for experimental work, however, these intervals might be needed to be even lower to capture the entire process.

Although the data acquisition delays were measured with the use of two python clock counters, data analysis showed minimal differences. Therefore, it was selected only “perf_counter” as it is also supposed to be the more accurate one (Dunn, 2015). Figure 4.2 illustrates a statistical description of acquisition delays in seconds. The data count numbers varied highly due to differences in processing time, but also the influence of acquisition delays. Looking at mean values, Markforged data provided the lowest mean of 0.146 seconds, Prusa with 0.312 while Ultimaker provided the highest of 1.123 acquisition delays. Considering the acquisition interval being 1 second and the mean of Ultimaker acquisition delays result in an average of over 2.1 seconds between each data captured. This also means that even if the acquisition interval was set to be 0, it would still take over 1 second to acquire the data. Standard deviation was also significantly higher for Ultimaker with 0.281, while Prusa and Markforged contained similar values of 0.032 and 0.033. This type of spread of data acquisition delays introduces uncertainty in the data acquisition process. In terms of maximal values, there were some extreme values that were chosen to keep during data analysis. This is due to the uncertainty of the true reason behind the anomalies in acquisition delays. A potential cause for such high values could be since a computer was used for regular tasks during the acquisition process, which might have impacted it. It also important to note the differences in data dimensionality, Markforged contained only 12 data types, Prusa 19, and Ultimaker 22. The result of these differences could have an impact on the acquisition delays as more data is being acquired.

Markforged

	timeperf_counter
count	31074.000000
mean	0.145605
std	0.032829
min	0.102166
25%	0.127896
50%	0.137853
75%	0.154943
max	2.154601

Ultimaker

	timeperf_counter
count	12647.000000
mean	1.123085
std	0.280933
min	0.571934
25%	0.943361
50%	1.085956
75%	1.251295
max	5.187223

Prusa

	timeperf_counter
count	23427.000000
mean	0.312333
std	0.032271
min	0.244564
25%	0.299237
50%	0.307873
75%	0.319541
max	3.482454

Figure 4.2: Statistical description of acquisition delays for each machine (unit in seconds)

4.3.2 Markforged data

As previously mentioned in 4.2.3, that Markforged data is quite limited, which provides only a single variable in terms of identifying process failure in form of hot end temperature. Looking at Markforged temperature data, statistical description in Figure 4.3 (a), it was observed that there were some occasions where temperature varied from 271 to 279 °C. It was investigated where these values occurred by looking at the current layer and time in the process, which provided an approximation of where in the process this occurred. Figure 4.3 (b) scatterplot illustrates where the more extreme values occurred based on the current layer, which was primarily at the start of the process. Additionally, the scatterplot illustrates the type of hot end temperature values that possible to acquire, which are integer numbers without any decimals behind them. Where the cause of only acquiring whole numbered data is primarily of limitations that the Eiger web interface provides. This type of temperature data might be less reliable as it is unknown if the decimals are rounded up or not, and hence the possible reason for high standard deviation of Markforged temperature. The more extreme values that occurred primarily during the start of the process were visualized. Figure 4.4 illustrates that this type of event occurred during every printing process.

	Hot_end_temperature
count	31074.000000
mean	274.591717
std	1.015395
min	271.000000
25%	274.000000
50%	274.000000
75%	275.000000
max	279.000000

(a)

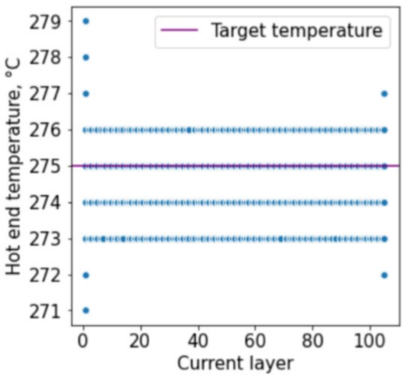

(b)

Figure 4.3: Hot end temperature data (a) statistical description, (b) scatter temperature during the process

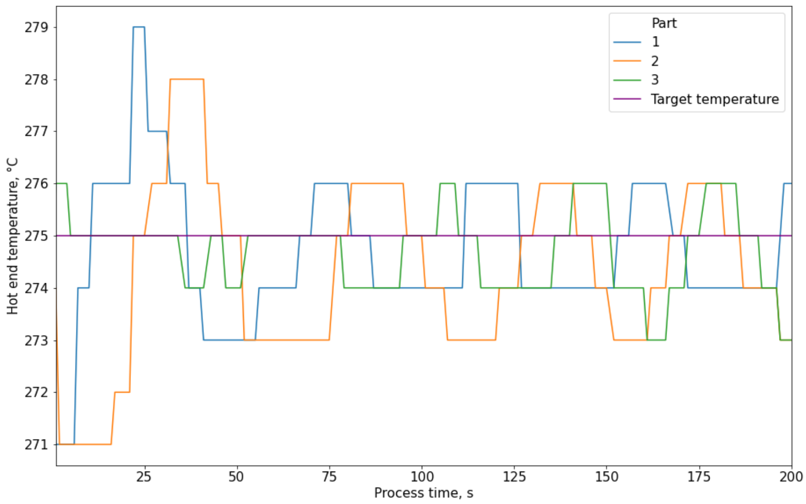

Figure 4.4: Hot end temperature data of extreme values and scatterplot of temperatures.

Moreover, during the printing and data acquisition process there occurred some challenges with data acquisition. Markforged acquisition utilizes Selenium Webdriver web scraping as a method. During the process, the chromedriver crashed several times, which resulted in the need of restarting the entire printing and acquisition process. However, the cause is error is unknown and was not observed during the testing phase.

4.3.3 Prusa data

Results of Prusa data showed that it contained extreme values, however, it seemed like it was natural process occurrence. Prusa statistical descriptions of temperature data are provided in Figure 4.5 (a). It was observed that the maximal hot end temperature deviated only with 1.6°C from the targeted temperature of 200°C. However, the minimal temperature significantly more deviated with 5.4°C from the targeted temperature. Therefore, during data analysis it was investigated where this event occurred and if it was a pattern. Due to data such as current layer in the process, fan speed, and process time, it was found when the event occurred and possible cause. Figure 4.5 (b) illustrates a scatterplot of all prints where these extreme minimum temperature values occurred, which was primarily during the second layer. This resulted in investigating further on what happens during the second layer. Figure 4.6 illustrates that this event occurs during the start of the second layer and occurred during every print. And as mentioned in section 3.4.2, that fan speed starts with 0% at the first layer and increases by 33% for every layer. Therefore, there is a potential that due to fan speed turning on to 33% it might have influenced the hot end temperature to drop, as the temperature quickly stabilizes back to the targeted temperature.

	Hot_end_temperature	Build_platform_temperature
count	23427.000000	23427.000000
mean	199.978678	60.014184
std	0.374475	0.121689
min	194.600000	59.300000
25%	199.800000	60.000000
50%	200.000000	60.000000
75%	200.200000	60.100000
max	201.600000	61.500000

(a)

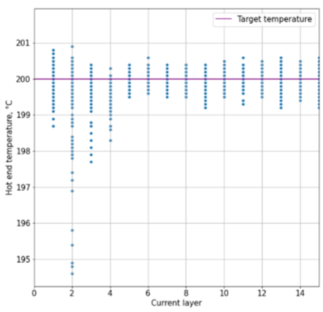

(b)

Figure 4.5 Temperature data (a) statistical description, (b) scatterplot of hot end temperature

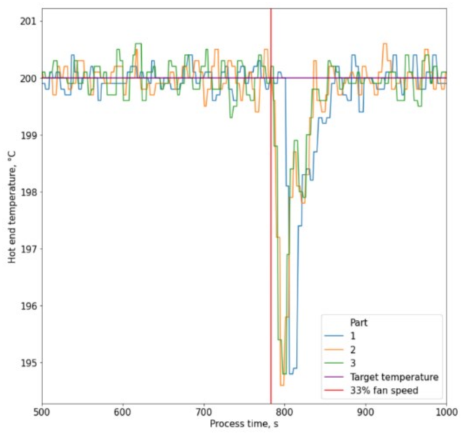

Figure 4.6: Hot end temperature changes during fan speed changes from 0 to 33%

Furthermore, Prusa Feed rate, which describes the speed of different movements in the XY-axis. All of the preset slicer settings of speed were identified there, however, some additional speeds were observed, which were unknown. Their occurrence showed to appear commonly during the process of each part. Additionally, these speeds were not identified anywhere in the slicing software, which could be a form of uncontrollable parameters generated by the slicer software.

4.3.4 Ultimaker data

Data from Ultimaker provided some anomalies in form of outliers and missing values. Outliers were detected during the printing process which showed that the temperature suddenly dropped from approximately the targeted temperature of 200°C to below 130°C and back to 200°C within few seconds, as illustrated in Figure 4.7. This event was only a single occurrence through all the printed objects, therefore it was chosen to exclude it from the dataset.

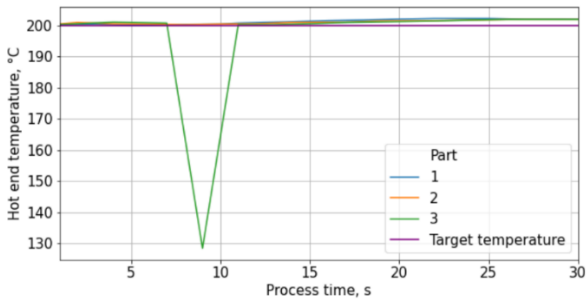

Figure 4.7: Ultimaker hot end temperature data anomaly

Additionally, some missing data was observed, in particular only for one data type, Z-axis coordinates. Missing values occurred during printing of all objects, in total 16 missing values. It was inspected where in the progress this event occurred by looking at data of process progress, part number, and time, it showed that these events occurred randomly, which is shown in Appendix 3. Therefore, the reason for this event is unknown. In terms of failure detection, Z coordinate variable could have significant importance as it identifies where in the process an event occurred. Although the progress of the process and time identify wherein the process it occurred, Ultimaker API does not contain layer data. Therefore Z coordinate is the only information that identifies where in form of height this event occurred.

However, the rows of missing z coordinate values were chosen to keep, due to the presence of other column data in these rows, and since it was not done any further analysis on Z-axis coordinate data. While, the temperature data of the build platform and hot end was used for statistical description, therefore it could have potentially impacted the results if they were to be removed. Where Figure 4.8 (a) provides with statistical description after the outlier had been removed, which shows that maximal and minimal values for hot end are somewhat stable around the targeted. Additionally, Figure 4.8 (b) illustrates a graph of hot end temperature of the same moment time frame as Figure 4.7.

	Hot_end_temperature	Build_platform_temperature
count	12646.000000	12646.000000
mean	199.987190	59.701508
std	0.228836	0.202283
min	198.100000	58.794445
25%	199.900000	59.571173
50%	200.000000	59.709189
75%	200.000000	59.845190
max	202.200000	60.468167

(a)

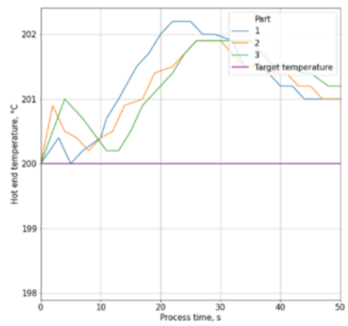

(b)

Figure 4.8 Temperature data after removed outlier (a) statistical description (b) line plot

Figure 4.9 (a) illustrates a scatterplot of hot end temperature, here the extreme values also occur during the early stages of the process. Whereas Figure 4.9 (b) illustrates the build platform temperatures during the process, which shows that most of the time the temperature was below the target. However, most of the data deviated within the range of 1°C of the targeted build platform temperature of 60°C.

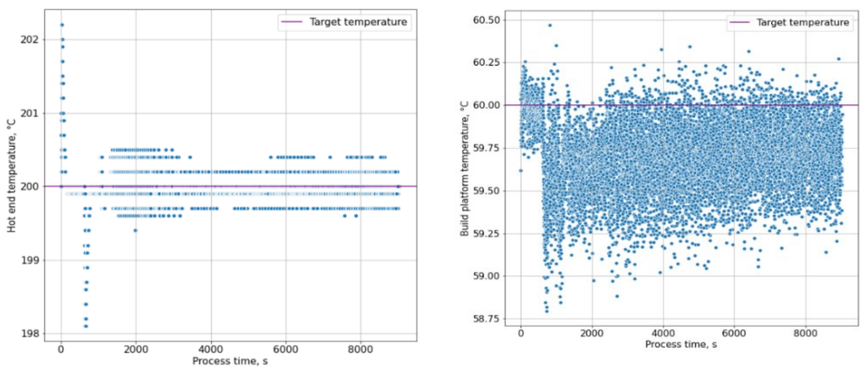

Figure 4.9: Scatterplots of (a) hot end temperature, (b) build platform temperature.

It was also analyzed if the same event as with Prusa occurs of hot end temperature dropping once fan speed changes. Figure 4.10 illustrates that this event occurs also with Ultimaker. However, the temperature drop is less significant, which is within 2°C of the targeted temperature, whereas, Prusa dropped below 5°C.

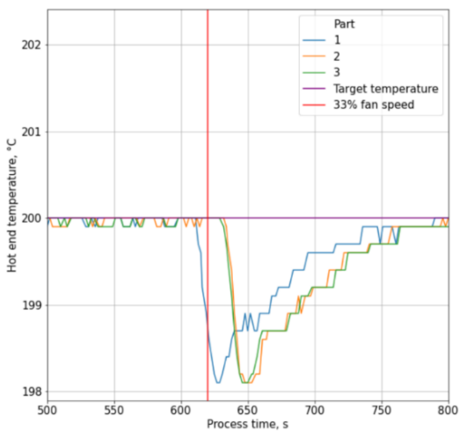

Figure 4.10 Hot end temperature changes during fan speed changes from 0 to 33%

Other data was also investigated, such as print head acceleration, and feeder data. Feeder data were static data that did not change during the process. However, it was not found any process parameters in slicing software that allowed control of these variables. Whereas with print head acceleration, all the preset acceleration parameters were identified during the process. However, just like with feed rate from Prusa, acceleration data contain some also unknown acceleration values. Nevertheless, these unknown acceleration values were only identified a total of 39 times of the 12465 data points collected.

4.3.5 Measurement data

Two groups of quality metrics in form of dimensional and geometric characteristics were measured. Geometric characteristic is represented as flatness and roundness. Dimensional characteristic is represented as a diameter. In total 3 parts were printed from each studied machine, where each part was measured three times to account for measurement errors. Figure 4.11 illustrates the measured errors in millimeters for each part characteristic. Where the measured error was calculated by subtracting the measured value from the targeted value for each characteristic. All measured parts from each machine contained some deviations between parts for the same characteristics. Markforged part 1 Figure 4.11 (a) roundness cylinder 16mm deviated considerably more from parts 2 and 3. Ultimaker Figure 4.11 (b) had the highest differences on the flatness of the base plate. Whereas Prusa Figure 4.11 (c) had also the highest deviation between parts on the flatness of the base plate.

Although sections 4.3.2, 4.3.3, and 4.3.4 presented some anomalies related to temperature deviation for each machine during the printing process, they occurred primarily at the earliest stages of the process. Highest and lowest temperatures occurred during the first 5 layers of the printing process. However, features of these layers were not measured, due to the fixture of the part to the CMM was covered . During later stages of the printing process, it was not observed any significant deviations between printed parts. Appendix 4 provides a statistical description of each part for each machine. In addition, it was compared with differences in process time between each part, as it could be assumed that the longer process time it takes, the finer quality would be of the parts. However, no relation was observed, therefore dimensional and geometrical features of FFF parts might require additional sensors.

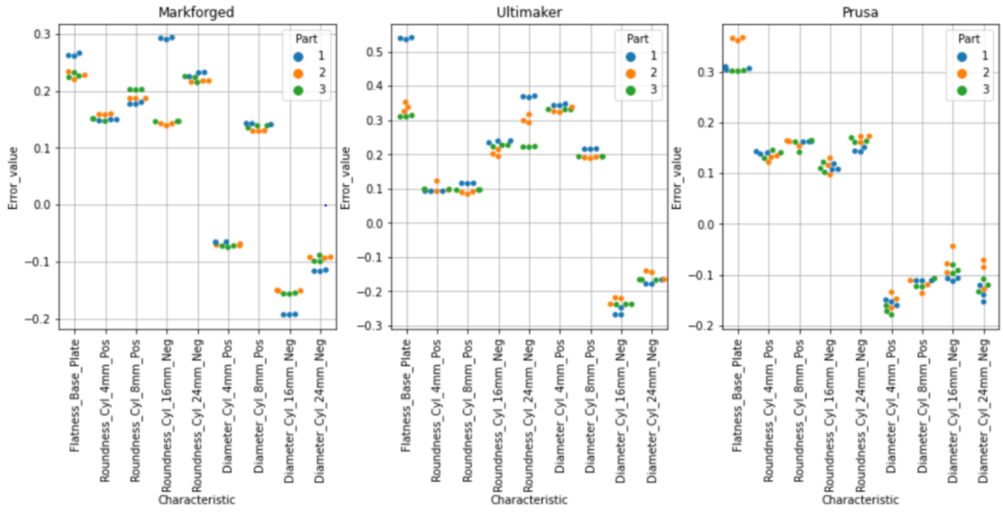

(a) (b) (c)

Figure 4.11: Measured error of features for each part, (a) Markforged, (b) Ultimaker, (c) Prusa.

5 Discussion

5.1 RQ1 Types of internal data in FFF machines

Although most of the research around the monitoring of FFF machines shows that they implement external sensors in order to obtain data about the process. The results of RQ1 showed that FFF machines are equipped with few sensors. Looking at each machine separately the most expensive machine Markforged contains the least amount of sensors, with only available temperature sensor for each hot end. However, it might be possible that Markforged contains internal sensing systems that were just not found through experimental work and in literature. This is because as mentioned in section 4.2.3 that machine was able to observe fiber hot end jams. While the less costly machines such as Prusa and Ultimaker contain considerably more sensors. This raises the question of why the cheaper machines contain more sensors. Therefore, in future work, it would be relevant to investigate the use of these sensors in terms of reliability. A possibility is that although some machines are equipped with more sensors, they might be prone to errors which could cause more harm than good in terms of failure detection. An example is that previously Ultimaker 3 contained a filament run-out sensor, and according to a member from the Ultimaker team, it caused errors which resulted in being removed from Ultimaker 3 (SandervG, 2017). Nonetheless, Prusa contained both an IR sensor and a mechanical lever to observe the presence of a filament. Considering FFF being a single-step process, running out of material would result in part being a waste and need of restart of the process.

Although all studied FFF machines require manual calibration to align the height of the nozzle to the build platform, it is not something that is done during each process, rather occasionally. Therefore, proximity sensor data identifies the approximate distance from the nozzle and build platform, during each process. Having the possibility to acquire proximity data could be important, as the machines contain mechanical parts, which could result in the manual calibrated alignment to deviate with time.

In addition to sensor data, it was presented that machines contain additional internal data. These data were in form of firmware data and G-code data. Where the G-code described the process and firmware data provide with positional data and machine configuration. Although data of firmware version and configuration was chosen to not be acquired, due to the primary focus on acquiring data of the process parameters. These data could have value in terms of identifying process failures, by providing additional information about machine and system. However, to access these data directly, there was a need to establish communication between FFF machine and computer, which was limited for both Markforged and Ultimaker. Nevertheless, Ultimaker provided some of these data through API. Where Markforged did not directly provide the possibility to access any form of data.

5.2 RQ2 Methods for acquiring data

The results of RQ2 showed that the studied machines which contained internal computer provide a possibility to access some data. Whereas machine such as Prusa which only had a control board, did not provide access to the data. This resulted in need for implementation of additional hardware and software, such as Raspberry Pi and OctoPrint. In addition to the studied FFF machines, OctoPrint supports many different types of consumer-grade FFF machines (OctoPrint, 2020). Therefore, there is a possibility that the same acquisition method would work on other FFF machines that support OctoPrint.

Although Ultimaker and Prusa with OctoPrint provide the same method of acquiring the data through API, the code for data acquisition is different. This is primarily due to the reason that it was not found a hierarchical structure to access specific resources of data for Prusa API. Instead, each time data was requested it was called for a list of resources where they had to be further processed to select the specific resources. Whereas Ultimaker API provided a structured way to access the specific resources relative to its origin API path. Nevertheless, both methods work, which firstly resulted in the choice of creating code of Ultimaker API as similar to Prusa. However, Ultimaker contained already high acquisition delays even by accessing the specific resources. When using the method of Prusa API for Ultimaker by accessing a list of data and then selecting out the specific resources of interest, the acquisition delays increased significantly more. This resulted in the choice of separating the API codes from Ultimaker and Prusa. Therefore, it is also important to note that if accessing specific resources was known or possible for Prusa API, it could potentially have reduced acquisition delays.

While Markforged machine did not provide any dedicated methods to acquire the data, although as mentioned in section 4.2.3 that Eiger uses API internally. However, they were not available for the users. This could potentially be the result of what has been mentioned in section 2.3.1 about API, which could come with a security threat. And since Markforged is greatly focused on information security as they are the only additive manufacturing company that has been ISO 27001 certified (Markforged, 2020c). Lastly, the possibility of generalizing data acquisition was presented, it showed that in order to generalize data acquisition for all machines, it would come with a cost of data quality. Nevertheless, looking broader at other FFF machines which provide API or support OctoPrint, could provide the possibility of generalizing the methods for data acquisition.

5.3 RQ3 Quality of acquired data

Looking at the data as a whole, it was possible to observe patterns and specific occurrences during the printing process. In terms of the development of predictive models, these patterns could provide the possibility to distinguish natural process occurrences from possible process failures. Additionally, it could be potentially possible to control unwanted process patterns with a combination of monitoring with predictive models and control systems for machines with API. As the API provides the possibility of not just acquiring the data, but also send data to control FFF machines through G-code commands.

In terms of identifying process failures with internal data, all machines provide hot end temperature data and some form of identifying where in the process they are. In the theoretical background, it was described several process failures related to temperature data. Although they were none of the failures were solely caused by hot end temperature, instead, it was a combination of different process parameters. Therefore, it is not possible to state that every studied machine could provide the possibility to identifying a specific process failure.

Moreover, Prusa and Ultimaker provided additional process parameter data, such as build platform temperature, fan speed, print speed, travel speed, and acceleration speeds. These data were also some of the key process parameters in terms of described process failures.

However, it is important to note that G-code data is just generated data from the slicer software, where the data acquisition captures these data at specific moments. Data such as feed rate, fan speed, and acceleration are parameters that the machine executes based on where in the process it is. Prusa provided with feed rate, however, it does provide acceleration, while Ultimaker provides the opposite. Although speed could be set to 60mm/s for a specific geometry, it does not indicate that the machine would reach that speed before moving on to another part of geometry with different set speeds. It is also unknown if the machines are accurate with these data, such as if the acceleration of 1000mm/s^2 is actually true or different value. Therefore, based on these types of data, it could be considered implementing external sensors such as optical with a vision system, especially since many described process failures show visual defects. The use of optical sensors allows the possibility of implementing to any FFF machines, without the need of modifying the machine or having as critical machine-specific sensor placement.

Furthermore, the acquired data for each machine was investigated and presented. It showed that feed rate and print head acceleration data contained additional variables which were not set by the user nor were they available in slicing software. These variables would need further studying in order to determine if these are uncontrollable parameters set by slicers or some errors. Additionally, Ultimaker API was the only of the studied machines which provided with missing and extreme values from the data acquisition process. These type of errors impacts the quality of the data.

Although acquisition delays were measured, they describe only the time it takes to acquire and store the data. It does not provide with any information on how synchronized the acquired data is compared to the actual sensor data. This is especially important for Markforged with use of web scraping methods. As you are completely limited to what data does web interface provide, which could have a large delay from the actual sensor data. Therefore, a possible future work would be investigating these aspects, as this would have a significant impact on the quality of the data.

The CMM measurement data of printed models were presented. Measurements of characteristics were compared between parts from the same machines. It was also investigated if the acquired data could capture the deviation between parts. However, results showed that it was not found any relation of printing data to the deviation between parts. Therefore, as future work, it could be considered to run the FFF process until failure during the data acquisition process. This would provide a more detailed understanding if the acquired data could identify some form of process failures. This would also provide an understanding in terms of the need for external sensors. A possible external sensor that could potentially have a significant impact on the monitoring of process failures would be a camera with a vision system. This is primarily due to that many of the listed process failures lead to some form of visual defects. But also when comparing to other sensors, such as vibration, thermocouple, etc. These sensors require strict specific placements on the FFF machine in order to provide accurate data. Whereas camera does not require as strict placement, which can result that this could be integrated into any FFF machine without the need of modifying any components on the machine.

6 Conclusion

The goal of this thesis is in introducing the possibility for acquiring internal data of studied FFF machines in order to provide the possibility for failure detection. As the research is primarily focused on failure detection through the use of external sensors. It introduces complexity in form of additional components, but also the potential of needing to modify machines, which could also become costly. Study findings showed FFF machines contain sensory data, but also additional data from internal communication with the machine. Where each studied machine provided some form of accessibility to the data, although, Prusa required additional hardware and software in order to access the data.

A data acquisition code was created for each machine based on what FFF machines provided, which included acquisition methods of web scraping and API. Markforged was the most closed machine and provided with only access through its cloud web interface. Whereas, Prusa and Ultimaker had both data on the web, but also provided with APIs to acquire data. Although the type of data varied from machine to machine, all machines provided with some process parameters that could have an impact on process failure, but also where the specific events occurred.

Data analysis was performed from the acquired data, where the goal was to investigate data quality. The acquisition delays showed that Markforged web scraping methods provided with the lowest acquisition delays. Ultimaker API had the highest acquisition delays. From all the studied machines, Markforged provided with the least possible data to acquire that were related to process failures. Hot end temperature was one of the process parameters that had an impact on many of the listed process failures. Ultimaker and Prusa provided with the possibility to observe not just temperature fluctuation, but also where it occurred and possible cause for fluctuation. Additionally, it was observed that although slicer software provides a large selection of process parameters, additional parameters were observed for feed rate and acceleration, which were not found anywhere in the slicer software. In terms of controlling the FFF process to avoid process failures, having control over all process parameters could be critical.

Although in the theoretical background it was described the types of failures that can occur due to different process parameters, and results identified the possible data to acquire. It has not been stated directly on what types of process failures it can identify, rather which it could potentially identify. This is because there is a need for further study in order to identify the potential of identifying the process failures. In addition, a recommendation of a possible external sensor, such as a camera could provide additional functionality in terms of identifying process failures. Which is a sensor that neither requires modifying machine nor very specific placement.

References

Abdullah, A. H. D. *et al.* (2019) Fabrication and Characterization Of Poly Lactic Acid (PLA)-Starch Based Bioplastic Composites, *IOP Conference Series: Materials Science and Engineering*. IOP Publishing, pp. 012052.

Adekanye, S. A. *et al.* (2017) Additive manufacturing: the future of manufacturing, *Additive Manufacturing*, 709, pp. 715.

Allen, R. J. and Trask, R. S. (2015) An experimental demonstration of effective Curved Layer Fused Filament Fabrication utilising a parallel deposition robot, *Additive Manufacturing*, 8, pp. 78-87.

Alrashed, T. *et al.* (2020) ScrAPIr: Making Web Data APIs Accessible to End Users, *Proceedings of the 2020 CHI conference on human factors in computing systems*. pp. 1-12.

Amza, C. G., Zapciu, A. and Popescu, D. (2017) Paste Extruder—Hardware Add-On for Desktop 3D Printers, *Technologies*, 5(3), pp. 50. Available at: https://www.mdpi.com/2227-7080/5/3/50.

Anderegg, D. A. *et al.* (2019) In-situ monitoring of polymer flow temperature and pressure in extrusion based additive manufacturing, *Additive Manufacturing*, 26, pp. 76-83. doi: https://doi.org/10.1016/j.addma.2019.01.002.

Aslanzadeh, S. *et al.* (2018) Investigation on electrical and mechanical properties of 3D printed nylon 6 for RF/microwave electronics applications, *Additive Manufacturing*, 21, pp. 69-75. doi: https://doi.org/10.1016/j.addma.2018.02.016.

Aw, Y. Y. *et al.* (2018) Effect of printing parameters on tensile, dynamic mechanical, and thermoelectric properties of FDM 3D printed CABS/ZnO composites, *Materials*, 11(4), pp. 466.

Baş, H., Elevli, S. and Yapıcı, F. (2019) Fault Tree Analysis for Fused Filament Fabrication Type Three-Dimensional Printers, *Journal of Failure Analysis and Prevention*, 19(5), pp. 1389-1400.

Bertoli, A. *et al.* (2021) Smart Node Networks Orchestration: A New E2E Approach for Analysis and Design for Agile 4.0 Implementation, *Sensors*, 21(5), pp. 1624.

Brenken, B. *et al.* (2018) Fused filament fabrication of fiber-reinforced polymers: A review, *Additive Manufacturing*, 21, pp. 1-16.

Brucker, A. D. and Herzberg, M. (2018) A formal model of the Document Object Model.

Bui, H. T. (2019) Toolpath planning methodology for multi-gantry fused filament fabrication 3d printing.

Camargo, J. C. *et al.* (2019) Mechanical properties of PLA-graphene filament for FDM 3D printing, *The International Journal of Advanced Manufacturing Technology*, 103(5), pp. 2423-2443.

Carolo, L. (2021) *2021 Best 3D Printer Controller Boards*. Available at: https://all3dp.com/2/3d-printer-controller-boards/ (Accessed: 04.06 2021).

Cavdir, D. (2020) Embedding Electronics in Additive Manufacturing for Digital Musical Instrument Design.

Chaulagain, R. S. *et al.* (2017) Cloud based web scraping for big data applications, *2017 IEEE International Conference on Smart Cloud (SmartCloud)*. IEEE, pp. 138-143.

Chen, X. *et al.* (2017) Restful API architecture based on laravel framework, *Journal of Physics: Conference Series*. IOP Publishing, pp. 012016.

Croom, B. P. *et al.* (2021) Mechanics of nozzle clogging during direct ink writing of fiber-reinforced composites, *Additive Manufacturing*, 37, pp. 101701. doi: https://doi.org/10.1016/j.addma.2020.101701.

Ćwikła, G. *et al.* (2017) The influence of printing parameters on selected mechanical properties of FDM/FFF 3D-printed parts, *IOP conference series: materials science and engineering*. IOP Publishing, pp. 012033.

Daid (2016) *Inside the Ultimaker 3 - Day 4 - Electronics*. Available at: https://community.ultimaker.com/topic/15649-inside-the-ultimaker-3-day-4-electronics/ (Accessed: 04.06 2021).

Dey, A. and Yodo, N. (2019) A systematic survey of FDM process parameter optimization and their influence on part characteristics, *Journal of Manufacturing and Materials Processing*, 3(3), pp. 64.
Di Paolo Emilio, M. (2013) *Data Acquisition Systems: From Fundamentals to Applied Design*. New York, NY: New York, NY: Springer New York.
Domingo-Espin, M. *et al.* (2018) Fatigue Performance of ABS Specimens Obtained by Fused Filament Fabrication, *Materials (Basel)*, 11(12), pp. 2521. doi: 10.3390/ma11122521.
Dongo, I. *et al.* (2020) *Web Scraping versus Twitter API: A Comparison for a Credibility Analysis*. Unpublished paper presented at Proceedings of the 22nd International Conference on Information Integration and Web-based Applications & Services. Chiang Mai, Thailand.
Duan, M., Yoon, D. and Okwudire, C. E. (2018) A limited-preview filtered B-spline approach to tracking control–With application to vibration-induced error compensation of a 3D printer, *Mechatronics*, 56, pp. 287-296.
Dunn, N. (2015) *Python Clocks Explained*. Available at: https://www.webucator.com/blog/2015/08/python-clocks-explained/ (Accessed: 06.06 2021).
Elkaseer, A., Schneider, S. and Scholz, S. G. (2020) Experiment-based process modeling and optimization for high-quality and resource-efficient FFF 3D printing, *Applied Sciences*, 10(8), pp. 2899.
Fu, T.-c. (2011) A review on time series data mining, *Engineering Applications of Artificial Intelligence*, 24(1), pp. 164-181.
Fu, Y. *et al.* (2020) In situ monitoring for fused filament fabrication process: A review, *Additive Manufacturing*, pp. 101749.
Fu, Y. *et al.* (2021) In situ monitoring for fused filament fabrication process: A review, *Additive Manufacturing*, 38, pp. 101749. doi: https://doi.org/10.1016/j.addma.2020.101749.
Galati, M. and Minetola, P. (2019) Analysis of Density, Roughness, and Accuracy of the Atomic Diffusion Additive Manufacturing (ADAM) Process for Metal Parts, *Materials*, 12(24), pp. 4122.
Gao, L., Zhang, C. and Sun, L. (2011) RESTful Web of Things API in sharing sensor data, *2011 International Conference on Internet Technology and Applications*. IEEE, pp. 1-4.
Gao, P. *et al.* (2018) {AIQL}: Enabling efficient attack investigation from system monitoring data, *2018 {USENIX} Annual Technical Conference ({USENIX}{ATC} 18)*. pp. 113-126.
Garcia, A. *et al.* (2010) ABS polymer electroless plating through a one-step poly (acrylic acid) covalent grafting, *ACS applied materials & interfaces*, 2(4), pp. 1177-1183.
García, B. *et al.* (2020) A survey of the selenium ecosystem, *Electronics*, 9(7), pp. 1067.
Ghosh, A. *et al.* (2019) High-temperature gas sensors for harsh environment applications: a review, *CLEAN–Soil, Air, Water*, 47(8), pp. 1800491.
Gibson, I. *et al.* (2014) *Additive manufacturing technologies*. Springer.
Gibson, I. *et al.* (2021) Material jetting *Additive Manufacturing Technologies.* Springer, pp. 203-235.
Gladen, M. and Staudt, V. (2020) Using a web scraping algorithm for component model generation in multiobjective optimization of power electronic applications, *2020 22nd European Conference on Power Electronics and Applications (EPE'20 ECCE Europe)*. IEEE, pp. P. 1-P. 10.
Greeff, G. P. and Schilling, M. (2018) Single print optimisation of fused filament fabrication parameters, *The International Journal of Advanced Manufacturing Technology*, 99(1), pp. 845-858.
Grimm, L., Pongratz, C. and Ehrlich, I. (2020) Grimm, Leopold Investigation of Continuous Fiber Filling Methods in Additively Manufactured Composites, *RARC 2020*, pp. 57.
Guo, Y.-X. *et al.* (2019) Differential Structure of Inductive Proximity Sensor, *Sensors*, 19(9), pp. 2210. Available at: https://www.mdpi.com/1424-8220/19/9/2210.

Harris, M. *et al.* (2019) Effect of material and process specific factors on the strength of printed parts in fused filament fabrication: A review of recent developments, *Materials*, 12(10), pp. 1664.
Häußge, G. (2017) *Why doesn't OctoPrint show me the current hotend position anywhere?* Available at: https://community.octoprint.org/t/why-doesnt-octoprint-show-me-the-current-hotend-position-anywhere/232 (Accessed: 10.05 2021).
Horvath, J. and Cameron, R. (2015) *3D Printing with MatterControl*. Apress : Imprint: Apress.
Hsiang Loh, G. *et al.* (2020) An overview of material extrusion troubleshooting, *Applied Sciences*, 10(14), pp. 4776.
Hu, Y. *et al.* (2018) Semantic information model and mobile smart device enabled data acquisition system for manufacturing workshop, *Journal of Physics: Conference Series*. IOP Publishing, pp. 012148.
Hunter, L. W. *et al.* (2020) Assessment of trapped powder removal and inspection strategies for powder bed fusion techniques, *The International Journal of Advanced Manufacturing Technology*, 106(9), pp. 4521-4532.
ISO/ASTM (2017) *Additive manufacturing - General principles - Terminology (ISO/ASTM 52900:2015)*. Available at: https://www.standard.no/no/Nettbutikk/produktkatalogen/Produktpresentasjon/?ProductID=913206 (Accessed: 04.03 2021).
Jacobson, D., Brail, G. and Woods, D. (2012) *APIs: A strategy guide*. " O'Reilly Media, Inc.".
JEMGHILI, R., TALEB, A. A. and MANSOURI, K. (2020) Additive Manufacturing Progress as a New Industrial Revolution, *2020 IEEE 2nd International Conference on Electronics, Control, Optimization and Computer Science (ICECOCS)*. IEEE, pp. 1-8.
Jin, Z., Zhang, Z. and Gu, G. X. (2019) Autonomous in-situ correction of fused deposition modeling printers using computer vision and deep learning, *Manufacturing Letters*, 22, pp. 11-15. doi: https://doi.org/10.1016/j.mfglet.2019.09.005.
Kabir, S., Mathur, K. and Seyam, A.-F. M. (2020) The road to improved Fiber-Reinforced 3D printing technology, *Technologies*, 8(4), pp. 51.
Kabir, S. M. F., Mathur, K. and Seyam, A.-F. M. (2020) The Road to Improved Fiber-Reinforced 3D Printing Technology, *Technologies*, 8(4), pp. 51. Available at: https://www.mdpi.com/2227-7080/8/4/51.
Kelly, B. *et al.* (2017) Computed Axial Lithography (CAL): Toward Single Step 3D Printing of Arbitrary Geometries, *arXiv preprint arXiv:1705.05893*.
Khan, M. F. *et al.* (2020) Real-time defect detection in 3D printing using machine learning, *Materials Today: Proceedings*.
Kohut, A. (2020) *Introducing Ultimaker Digital Factory*. Available at: https://ultimaker.com/learn/introducing-ultimaker-digital-factory (Accessed: 04.06 2021).
Korkees, F., Allenby, J. and Dorrington, P. (2020) 3D printing of composites: design parameters and flexural performance, *Rapid prototyping journal*, 26(4), pp. 699-706. doi: 10.1108/RPJ-07-2019-0188.
Kretzschmar, N. *et al.* (2018) Evaluating the readiness level of additively manufactured digital spare parts: An industrial perspective, *Applied Sciences*, 8(10), pp. 1837.
Kuznetsov, V. E., Tavitov, A. G. and Urzhumtcev, O. D. (2019) Hardware factors influencing interlayer bonding strength of parts obtained by Fused Filament Fabrication.
Kuznetsov, V. E. *et al.* (2019) Desktop Fabrication of Strong Poly (Lactic Acid) Parts: FFF Process Parameters Tuning, *Materials*, 12(13), pp. 2071. Available at: https://www.mdpi.com/1996-1944/12/13/2071.
Lai, Y. *et al.* (2018) Fog-based two-phase event monitoring and data gathering in vehicular sensor networks, *Sensors*, 18(1), pp. 82.
Leirmo, T. and Martinsen, K. (2019a) *Deterministic part orientation in additive manufacturing using feature recognition*.

Leirmo, T. and Martinsen, K. (2019b) *Evolutionary algorithms in additive manufacturing systems: Discussion of future prospects*.
Leirmo, T., Semeniuta, O. and Martinsen, K. (2020) *Tolerancing from STL data: A Legacy Challenge*.
Leirmo, T. L. and Semeniuta, O. (2021) Investigating the Dimensional and Geometric Accuracy of Laser-Based Powder Bed Fusion of PA2200 (PA12): Experiment Design and Execution, *Applied Sciences*, 11(5), pp. 2031. Available at: https://www.mdpi.com/2076-3417/11/5/2031.
Li, Y. *et al.* (2019) In-Situ Monitoring and Diagnosing for Fused Filament Fabrication Process Based on Vibration Sensors, *Sensors*, 19(11), pp. 2589. Available at: https://www.mdpi.com/1424-8220/19/11/2589.
Li, Z. *et al.* (2019) Prediction of surface roughness in extrusion-based additive manufacturing with machine learning, *Robotics and Computer-Integrated Manufacturing*, 57, pp. 488-495. doi: https://doi.org/10.1016/j.rcim.2019.01.004.
Ligon, S. C. *et al.* (2017) Polymers for 3D Printing and Customized Additive Manufacturing, *Chem. Rev*, 117(15), pp. 10212-10290. doi: 10.1021/acs.chemrev.7b00074.
Liu, C. *et al.* (2019) Image analysis-based closed loop quality control for additive manufacturing with fused filament fabrication, *Journal of Manufacturing Systems*, 51, pp. 75-86. doi: https://doi.org/10.1016/j.jmsy.2019.04.002.
Liu, X. F. *et al.* (2016) Implementation of MTConnect for open source 3D printers in cyber physical manufacturing cloud, *International Design Engineering Technical Conferences and Computers and Information in Engineering Conference*. American Society of Mechanical Engineers, pp. V01AT02A019.
Liu, Z., Lei, Q. and Xing, S. (2019) Mechanical characteristics of wood, ceramic, metal and carbon fiber-based PLA composites fabricated by FDM, *Journal of Materials Research and Technology*, 8(5), pp. 3741-3751. doi: https://doi.org/10.1016/j.jmrt.2019.06.034.
Lu, Y. and Wang, Y. (2019) An efficient transient temperature monitoring of fused filament fabrication process with physics-based compressive sensing, *IISE Transactions*, 51(2), pp. 168-180.
Malekipour, E., Attoye, S. and El-Mounayri, H. (2018) Investigation of Layer Based Thermal Behavior in Fused Deposition Modeling Process by Infrared Thermography, *Procedia Manufacturing*, 26, pp. 1014-1022. doi: https://doi.org/10.1016/j.promfg.2018.07.133.
Maleshkova, M., Pedrinaci, C. and Domingue, J. (2010) Investigating web apis on the world wide web, *2010 eighth ieee european conference on web services*. IEEE, pp. 107-114.
Markforged (2020a) *Fiber Jam Troubleshooting (Desktop)*. Available at: https://support.markforged.com/portal/s/article/Fiber-Jam-Detection-Desktop (Accessed: 10.05 2021).
Markforged (2020b) *Checking Electronics Connections*. Available at: https://support.markforged.com/portal/s/article/Checking-Electronics-Connections (04.06).
Markforged (2020c) *Markforged Achieves ISO/IEC 27001 Certification*. Available at: https://markforged.com/resources/news-events/iso-certification (Accessed: 25.04 2021).
Markforged (2020d) *Prepare the Print Bed (Desktop)*. Available at: https://support.markforged.com/portal/s/article/Prepare-the-Print-Bed-Desktop (Accessed: 05.05 2021).
Markforged (2020e) *Onyx*. Available at: https://support.markforged.com/portal/s/article/Onyx (Accessed: 04.05 2021).
Markforged (2021) *Security at*

Markforged. Available at: http://static.markforged.com/downloads/MarkforgedSecurityWhitepaper.pdf?mfa=linkedin (Accessed: 25.04 2021).

Márquez, F. P. G. *et al.* (2012) Condition monitoring of wind turbines: Techniques and methods, *Renewable Energy*, 46, pp. 169-178.
Medellín-Castillo, H. and Zaragoza-Siqueiros, J. (2019) Design and Manufacturing Strategies for Fused Deposition Modelling in Additive Manufacturing: A Review, *Chinese Journal of Mechanical Engineering*, 32. doi: 10.1186/s10033-019-0368-0.
Mendricky, R. and Fris, D. (2020) Analysis of the Accuracy and the Surface Roughness of FDM/FFF Technology and Optimisation of Process Parameters, *Tehnički vjesnik*, 27(4), pp. 1166-1173.
Mertens, W. (2017) *Quantitative data analysis*. Springer.
Miller, D. (2021) *Best Direct Drive 3D Printer*. Available at: https://io3dprint.com/best-direct-drive-3d-printer/ (Accessed: 28.05 2021).
Mohamed, O. A. *et al.* (2016) Effect of process parameters on dynamic mechanical performance of FDM PC/ABS printed parts through design of experiment, *Journal of materials engineering and performance*, 25(7), pp. 2922-2935.
Moretti, M., Bianchi, F. and Senin, N. (2020a) Towards the development of a smart fused filament fabrication system using multi-sensor data fusion for in-process monitoring, *Rapid prototyping journal*.
Moretti, M., Bianchi, F. and Senin, N. (2020b) Towards the development of a smart fused filament fabrication system using multi-sensor data fusion for in-process monitoring, *Rapid prototyping journal*, 26(7), pp. 1249-1261. doi: 10.1108/RPJ-06-2019-0167.
Mwema, F. M. and Akinlabi, E. T. (2020) *Fused Deposition Modeling: Strategies for Quality Enhancement*. Cham: Cham: Springer International Publishing AG.
Needs, S. H. *et al.* (2019) Exploiting open source 3D printer architecture for laboratory robotics to automate high-throughput time-lapse imaging for analytical microbiology, *PloS one*, 14(11), pp. e0224878.
OctoPrint (2020) *Printers known to work/not work*. Available at: https://community.octoprint.org/t/printers-known-to-work-not-work/21147/1 (Accessed: 28.05 2021).
OllisGit (2021) *OctoPrint-DisplayLayerProgress*. Available at: https://github.com/OllisGit/OctoPrint-DisplayLayerProgress (Accessed: 30.04 2021).
Osswald, T. A., Puentes, J. and Kattinger, J. (2018) Fused filament fabrication melting model, *Additive Manufacturing*, 22, pp. 51-59. doi: https://doi.org/10.1016/j.addma.2018.04.030.
Patil, R. and Temkar, R. (2017) Intelligent Testing Tool: Selenium Web Driver, *International Research Journal of Engineering and Technology (IRJET) Volume*, 4.
Peterson, A. M. (2019) Review of acrylonitrile butadiene styrene in fused filament fabrication: A plastics engineering-focused perspective, *Additive Manufacturing*, 27, pp. 363-371. doi: https://doi.org/10.1016/j.addma.2019.03.030.
Prusa Research (2021) *Original Prusa i3 MK3S+ kit*. Available at: https://shop.prusa3d.com/en/3d-printers/180-original-prusa-i3-mk3s-kit.html (Accessed: 04.06 2021).
Raghavendra, S. (2021) Introduction to Selenium *Python Testing with Selenium.* Springer, pp. 1-14.
Ramya, P., Sindhura, V. and Sagar, P. V. (2017) Testing using selenium web driver, *2017 Second International Conference on Electrical, Computer and Communication Technologies (ICECCT)*. IEEE, pp. 1-7.
Rao, P. K. *et al.* (2015) Online real-time quality monitoring in additive manufacturing processes using heterogeneous sensors, *Journal of manufacturing science and engineering*, 137(6).
Rathee, S. *et al.* (2017) Effect of varying spatial orientations on build time requirements for FDM process: A case study, *Defence technology*, 13(2), pp. 92-100.
Ravi, P. and Shiakolas, P. S. (2021) Effects of slicing parameters on measured fill density for 3D printing of precision cylindrical constructs using Slic3r, *SN Applied Sciences*, 3(3), pp. 1-10.

RepRap (2021) *G-code*. Available at: https://reprap.org/wiki/G-code (Accessed: 26.04 2021).
Research, P. (2021) *IR Filament Sensor Troubleshooting (MK2.5S, MK3S)*. Available at: https://help.prusa3d.com/en/article/ir-filament-sensor-troubleshooting-mk2-5s-mk3s_112226 (Accessed: 27.05 2021).
Saboori, A. *et al.* (2019) Application of Directed Energy Deposition-Based Additive Manufacturing in Repair, *Applied Sciences*, 9(16), pp. 3316. Available at: https://www.mdpi.com/2076-3417/9/16/3316.
Saluja, A., Xie, J. and Fayazbakhsh, K. (2020) A closed-loop in-process warping detection system for fused filament fabrication using convolutional neural networks, *Journal of Manufacturing Processes*, 58, pp. 407-415. doi: https://doi.org/10.1016/j.jmapro.2020.08.036.
SandervG (2017) *Filament monitor for UM3/UM3E*. Available at: https://community.ultimaker.com/topic/19790-filament-monitor-for-um3um3e/ (Accessed: 27.05 2021).
Shaqour, B. *et al.* (2021) Gaining a better understanding of the extrusion process in fused filament fabrication 3D printing: a review, *The International Journal of Advanced Manufacturing Technology*, pp. 1-13.
Shembekar, A. V. *et al.* (2018) Trajectory planning for conformal 3d printing using non-planar layers, *International Design Engineering Technical Conferences and Computers and Information in Engineering Conference*. American Society of Mechanical Engineers, pp. V01AT02A026.
Shen, H., Sun, W. and Fu, J. (2019) Multi-view online vision detection based on robot fused deposit modeling 3D printing technology, *Rapid prototyping journal*.
SIMPLIFY3D (2021) *Layer Shifting*. Available at: https://www.simplify3d.com/support/print-quality-troubleshooting/layer-shifting/ (Accessed: 13.05 2021).
Singrodia, V., Mitra, A. and Paul, S. (2019) A Review on Web Scrapping and its Applications, *2019 International Conference on Computer Communication and Informatics (ICCCI)*. IEEE, pp. 1-6.
Sirojan, T., Phung, T. and Ambikairajah, E. (2018) Enabling Deep Learning on Embedded Systems for IoT Sensor Data Analytics: Opportunities and Challenges, *2018 IEEE International Conference on Information and Automation for Sustainability (ICIAfS)*, *21-22 Dec. 2018*. pp. 1-5.
Soman, R. *et al.* (2019) A Study of Sensor Placement Optimization Problem for Guided Wave-Based Damage Detection, *Sensors*, 19(8), pp. 1856. Available at: https://www.mdpi.com/1424-8220/19/8/1856.
Soriano Heras, E. *et al.* (2018) Filament advance detection sensor for fused deposition modelling 3D printers, *Sensors*, 18(5), pp. 1495.
Spreeman, M. E., Stretz, H. A. and Dadmun, M. D. (2019) Role of compatibilizer in 3D printing of polymer blends, *Additive Manufacturing*, 27, pp. 267-277. doi: https://doi.org/10.1016/j.addma.2019.03.009.
Steuben, J., Van Bossuyt, D. L. and Turner, C. (2015) Design for fused filament fabrication additive manufacturing, *International Design Engineering Technical Conferences and Computers and Information in Engineering Conference*. American Society of Mechanical Engineers, pp. V004T005A050.
Sumalatha, A., Vookanti, R. and Vannala, S. (2021) Study on Applications of SQL and Not only SQL Databases used for Big Data Analytics, *INTERNATIONAL JOURNAL FOR RESEARCH & DEVELOPMENT IN TECHNOLOGY*, 15, pp. 127-130.
Surwase, V. (2016) REST API modeling languages-a developer's perspective, *Int. J. Sci. Technol. Eng*, 2(10), pp. 634-637.
Syafrudin, M. *et al.* (2018) Performance Analysis of IoT-Based Sensor, Big Data Processing, and Machine Learning Model for Real-Time Monitoring System in Automotive Manufacturing, *Sensors*, 18(9), pp. 2946. Available at: https://www.mdpi.com/1424-8220/18/9/2946.

Tagami, T. *et al.* (2017) 3D printing factors important for the fabrication of polyvinylalcohol filament-based tablets, *Biological and Pharmaceutical Bulletin*, 40(3), pp. 357-364.

Tantillo, A. G. (2019) Annealing of Fused Filament Fabricated Nylon 6 with Elevated Isostatic Pressure.

Tao, F. *et al.* (2018) Data-driven smart manufacturing, *Journal of Manufacturing Systems*, 48, pp. 157-169. doi: https://doi.org/10.1016/j.jmsy.2018.01.006.

Tlegenov, Y., Hong, G. S. and Lu, W. F. (2018) Nozzle condition monitoring in 3D printing, *Robotics and Computer-Integrated Manufacturing*, 54, pp. 45-55.

Tlegenov, Y., Lu, W. F. and Hong, G. S. (2019) A dynamic model for current-based nozzle condition monitoring in fused deposition modelling, *Progress in Additive Manufacturing*, 4(3), pp. 211-223.

Todd, M. D. (2014) 2 - Sensor data acquisition systems and architectures, in Wang, M. L., Lynch, J. P. and Sohn, H. (ed.) *Sensor Technologies for Civil Infrastructures.* Woodhead Publishing, pp. 23-56.

Ultimaker (2020a) *How to fix pillowing*. Available at: https://support.ultimaker.com/hc/en-us/articles/360012016240-How-to-fix-pillowing (Accessed: 12.04 2021).

Ultimaker (2020b) *Speed settings*. Available at: https://support.ultimaker.com/hc/en-us/articles/360012611079-Speed-settings (Accessed: 29.05 2021).

Ultimaker (2020c) *How to fix under-extrusion*. Available at: https://support.ultimaker.com/hc/en-us/articles/360012112859-How-to-fix-under-extrusion (Accessed: 12.04 2021).

Ultimaker (2020d) *How to fix warping*. Available at: https://support.ultimaker.com/hc/en-us/articles/360012113239-How-to-fix-warping (Accessed: 12.04 2021).

Ultimaker (2020e) *How to fix stringing*. Available at: https://support.ultimaker.com/hc/en-us/articles/360012016280-How-to-fix-stringing (Accessed: 12.04 2021).

Ultimaker (2021) *Ultimaker printer APIs*. Available at: https://support.ultimaker.com/hc/en-us/articles/360021076960-Ultimaker-printer-APIs (Accessed: 04.06 2021).

van Bracht, R., Kleer, R. and Piller, F. (2017) Predicting the future of additive manufacturing: A Delphi study on economic and societal implications of 3D printing for 2030, *Technological Forecasting and Social Change*, 117. doi: 10.1016/j.techfore.2017.01.006.

Vosynek, P. *et al.* (2018) Influence of process parameters of printing on mechanical properties of plastic parts produced by FDM 3D printing technology, *MATEC web of conferences*. EDP Sciences, pp. 02014.

Wang, Y. *et al.* (2019) CryptSQLite: SQLite with high data security, *IEEE Transactions on Computers*, 69(5), pp. 666-678.

Wong, S. Y., Chuah, J. H. and Yap, H. J. (2020) Technical data-driven tool condition monitoring challenges for CNC milling: a review, *The International Journal of Advanced Manufacturing Technology*, 107, pp. 4837-4857.

Wu, D. *et al.* (2020) Data-driven approach to application programming interface documentation mining: A review, *Wiley Interdisciplinary Reviews: Data Mining and Knowledge Discovery*, 10(5), pp. e1369.

Wu, H., Wang, Y. and Yu, Z. (2016) In situ monitoring of FDM machine condition via acoustic emission, *The International Journal of Advanced Manufacturing Technology*, 84(5-8), pp. 1483-1495.

Wu, H., Yu, Z. and Wang, Y. (2019) Experimental study of the process failure diagnosis in additive manufacturing based on acoustic emission, *Measurement*, 136, pp. 445-453. doi: https://doi.org/10.1016/j.measurement.2018.12.067.

Xiao, W., Huang, H. and Zhao, G. (2018) Communication methodology between machine tools using MTConnect protocol, *MATEC web of conferences*, 175, pp. 03066. doi: 10.1051/matecconf/201817503066.

Yi, D.-H., Lee, T.-J. and Cho, D.-I. D. (2018) A New Localization System for Indoor Service Robots in Low Luminance and Slippery Indoor Environment Using Afocal Optical Flow Sensor Based Sensor Fusion, *Sensors (Basel)*, 18(1), pp. 171. doi: 10.3390/s18010171.

Zapciu, A., Tasca, G. and Amza, C. (2018) Considerations on 3D printing joints parts, *IOP Conference Series: Materials Science and Engineering*. IOP Publishing, pp. 022061.

Appendices

Appendix 1: Ultimaker Camera perspective and quality

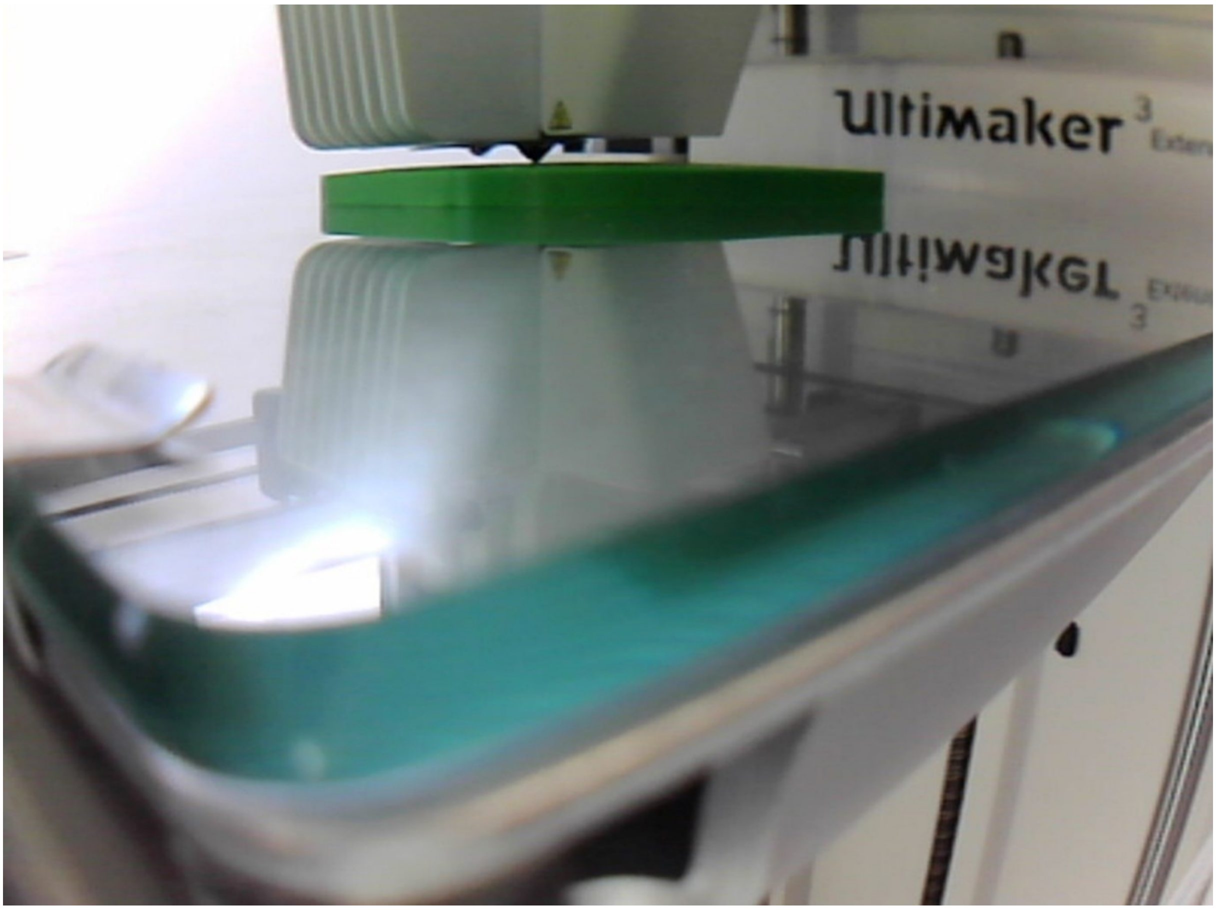

Appendix 2: Comparison of available data between each studied FFF machine

Data	Ultimaker 3 Extended	Original Prusa i3 MK3S	Markforged Mark Two
Current Hot end temperature	X	X	X
Target hot end temperature	X	X	
Current Build platform Temperature	X	X	
Target Build platform temperature	X	X	
Machine state	X	X	X
Current layer		X	X
Total layer		X	X
Z coordinate	X	X	
Fan speed	X	X	
Process progress	X	X	
Feed rate		X	
Material in use			X
User		X	X
Process time left			X
Process time		X	
XY - position	X		
Object	X	X	X
Average layer duration		X	
Last layer duration		X	
Head acceleration	X		
Hot end material extruded	X		
Hot end time spent hot	X		
Hot end max temperature exposed	X		
Z-axis offset	X		
Feeder jerk	X		

Feeder acceleration	X		
Feeder max speed	X		

Appendix 3: Ultimaker API missing values of Z coordinates

	Date	Progress	Z_coordinate	X_coordinate	Y_coordinate	Part
1126	2021-05-10 10:32:31	0.270116	NaN	65.603	89.26	1
1603	2021-05-10 10:50:16	0.389526	NaN	138.545	138.053	1
2408	2021-05-10 11:20:07	0.585276	NaN	130.683	86.821	1
3409	2021-05-10 11:56:50	0.832806	NaN	104.426	108.44	1
3886	2021-05-10 12:14:20	0.949331	NaN	72.836	104.315	1
4499	2021-05-10 12:42:30	0.094451	NaN	134.882	83.008	2
6544	2021-05-10 13:49:27	0.535727	NaN	131.865	123.479	2
6926	2021-05-10 14:01:41	0.615686	NaN	91.738	114.775	2
7097	2021-05-10 14:07:07	0.651439	NaN	75.477	99.676	2
8157	2021-05-10 14:45:46	0.911056	NaN	75.083	115.832	2
9608	2021-05-10 15:44:47	0.253165	NaN	91.255	88.116	3
11163	2021-05-10 16:42:02	0.632362	NaN	95.001	118.495	3
11474	2021-05-10 16:53:19	0.707998	NaN	86.844	80.258	3
11851	2021-05-10 17:07:14	0.803735	NaN	69.191	102.588	3
12276	2021-05-10 17:23:01	0.909237	NaN	95.203	119.387	3
12444	2021-05-10 17:29:13	0.950489	NaN	126.946	83.301	3

Appendix 4: Printing data for each machine, includes process time and statistical description for each part

Prusa

	Part1	Part2	Part3
Total process time (s)	10460.000000	10481.000000	10495.000000
Hot end temperature°C mean	199.978133	199.975692	199.982216
Hot end temperature°C min	194.800000	194.600000	194.800000
Hot end temperature°C max	201.400000	201.600000	201.600000
Hot end temperature°C std	0.372731	0.377690	0.373003
Build platform temperature°C max	59.400000	59.500000	59.300000
Build platform temperature°C min	60.900000	61.300000	61.500000
Build platform temperature°C std	0.109405	0.124488	0.130159

Ultimaker

	Part1	Part2	Part3
Total process time (s)	8999.000000	9034.000000	8988.000000
Hot end temperature°C mean	199.986807	199.988580	199.986075
Hot end temperature°C min	198.100000	198.100000	198.100000
Hot end temperature°C max	202.200000	201.900000	201.900000
Hot end temperature°C std	0.228455	0.225908	0.232362
Build platform temperature°C max	58.905377	58.819473	58.794445
Build platform temperature°C min	60.313894	60.468167	60.348769
Build platform temperature°C std	0.192475	0.207069	0.206489

Markforged

	Part1	Part2	Part3
Total process time (s)	12179.000000	12181.000000	12181.000000
Hot end temperature°C mean	274.671858	274.542915	274.542915
Hot end temperature°C min	271.000000	271.000000	273.000000
Hot end temperature°C max	279.000000	278.000000	276.000000
Hot end temperature°C std	0.897167	1.086232	1.048915

NTNU
Norwegian University of
Science and Technology